Extended droplet theory for aging in short-range spin glasses and a numerical examination

Hajime Yoshino*
Department of Earth and Space Science, Faculty of Science, Osaka University, Toyonaka, Osaka 560-0043, Japan

Koji Hukushima† and Hajime Takayama‡
Institute for Solid State Physics, University of Tokyo, 5-1-5 Kashiwa-no-ha, Kashiwa, Chiba 277-8581, Japan
(Received 20 March 2002; published 30 August 2002)

We analyze isothermal aging of a four-dimensional Edwards-Anderson model in detail by Monte Carlo simulations. We analyze the data in the view of an extended version of the droplet theory proposed recently which is based on the original droplet theory plus conjectures on the anomalously soft droplets in the presence of domain walls. We found that the scaling laws including some fundamental predictions of the original droplet theory explain our results well. The results of our simulation strongly suggest the separation of the breaking of the time translational invariance and the fluctuation dissipation theorem in agreement with our scenario.

DOI: 10.1103/PhysRevB.66.064431 PACS number(s): 75.50.Lk, 75.10.Nr, 75.40.Gb

I. INTRODUCTION

Spin glasses exhibit characteristic slow dynamics below the spin-glass (SG) transition temperature T_c. Recently aging phenomena, which have been known for a long time in glassy systems,[1] has attracted renewed interest both in experimental and theoretical studies.[2–7] A major theoretical progress was the development of the dynamical mean-field theories (MFT) of spin glasses and related systems.[8] Most remarkably it found that the field cooled (FC) susceptibility $\chi_{\rm FC}$ is larger than the equilibrium susceptibility $\chi_{\rm EA}$ which is related to the Edwards-Anderson (EA) order parameter $q_{\rm EA}$ by the fluctuation dissipation theorem (FDT) as $k_BT\chi_{\rm EA}=1-q_{\rm EA}$. This finding corresponds to the well known experimental observation[9] that $\chi_{\rm FC}$ is *larger* than the zero field cooled (ZFC) susceptibility $\chi_{\rm ZFC}$. In addition, many new view points for the glassy dynamics were discovered subsequently such as the concept of effective temperature.[10,11] However, the MFT does not provide insights into what will become important in realistic finite dimensional systems. Most seriously, thermally activated nucleation processes which are presumably important in finite dimensional glassy systems cannot be captured at the mean-field level.

Recently we proposed a refined scenario[12] for the isothermal aging based on the droplet theory for spin glasses.[13–15] We conjectured that the original idea of effective stiffness of droplets in the presence of frozen-in domain wall, introduced by Fisher and Huse,[15] can be extended to take into account anomalously soft droplet excitations which are as large as frozen-in extended defects, i.e., domain walls. This conjecture is partly motivated by the results of recent active studies of spin-glass models at $T=0$[16] which revealed existence of anomalous low-energy and large scale excitations. The anomalously soft droplets allow emergence of a new dynamical order parameter q_D and the dynamical susceptibility χ_D associated with the former by FDT $k_BT\chi_D=1-q_D$. The dynamical order parameter q_D is expected to be *smaller* than the equilibrium EA order parameter $q_{\rm EA}$ which means that the dynamical susceptibility χ_D is *larger* than the equilibrium susceptibility $\chi_{\rm EA}$. Consequently, our scenario implies a novel feature that breaking of the time translational invariance (TTI) and FDT separates asymptotically at large length (time) scales: the breaking point of TTI converges to the equilibrium EA order parameter $q_{\rm EA}$ while that of FDT converges to the new dynamical order parameter q_D smaller than $q_{\rm EA}$. We will find that $\chi_{\rm FC}=\chi_D$ so that our scenario also suggests $\chi_{\rm FC}>\chi_{\rm EA}$.

Both the original droplet theory[15] and our refined scenario[12] predict scaling laws for the time-dependent quantities measured in aging such as the magnetic autocorrelation function and the dynamical susceptibilities in terms of a time-dependent length scale $L(t)$ which presumably grows extremely slowly in a logarithmic fashion due to thermally activated processes. By now it is well understood that length scale that can be explored in practice is very much limited not only in numerical simulations (typically $1-10$ lattice spacings) but also in real experiments (typically ~ 100 lattice spacings). The latter implies one must seriously take care possible preasymptotic behaviors to elucidate the desired asymptotic behavior associated with the putative $T=0$ glassy fixed point. To cope with such a complicated situation still in a controlled way, we examine the scaling theory by Monte Carlo simulations in two strokes.

First, we examine the growth law of the dynamical length scale $L(t)$ itself by directly measuring the spatial coherence using two real replicas. As realized in recent studies,[17–20] the problem of crossover from critical to activated dynamics is the central issue here. Second, we examine the scaling properties of the time-dependent quantities of our interest by parametrizing the times using the data of the time-dependent length scale obtained by the separate simulation. The original droplet theory and our extended version provide some useful information of finite *length* correction terms to the asymptotic limit $L\to\infty$. The two-strokes (or parametric) strategy of the present paper, which is already employed partially in the previous studies,[17,21–24] allows us to cope with the mixture preasymptotic behaviors of different origins in a controlled way and far more advantages than usual approaches which try to examine the scaling laws in one stroke directly as a function of times blindly with many uncontrolled fitting parameters.

In this paper we present a detailed study on the isothermal

aging by Monte Carlo (MC) simulations on a four-dimensional (4D) EA Ising SG model. While the model system in 4D is somewhat nonrealistic, the advantage of studying the 4D Ising EA model is that important equilibrium properties concerning both the critical phenomena at T_c and some essential scaling properties associated with the $T=0$ glassy fixed point, both of which will turn out to provide extremely useful information to study off-equilibrium dynamics, are far better known in 4D than in three dimensions (3D). In oder to take care of the critical fluctuations, we will use the well established information provided by the previous studies. Furthermore the value of stiffness exponent θ is found to be considerably larger than that of 3D which implies easier access to low-temperature properties in 4D than in 3D within limited length scales. Indeed, a recent analysis of defect free-energy in 4D could clarify the anticipated crossover from critical regime to low-temperature regime.[25] In our analysis we employ the values of these parameters and fix them so that we are left with a few free parameters in our scaling analysis.

The present paper is organized as follows. In the next section we introduce our model system studied. In Sec. III, we introduce the two time quantities used in this paper and summarize some of their basic properties for the convenience of later sections. In Sec. IV we explain our extended droplet scaling theory[12] in a more self-contained and comprehensive manner recalling also the fundamental results of the original droplet theory.[13–15] In Sec. V we examine the growth law of the dynamical length $L(t)$ by MC simulations. In Secs. VI and VII, we examine time-dependent physical quantities by MC simulations and perform scaling analysis using the growth law $L(t)$ obtained in Sec. V. A part of the results was already reported in Ref. 17. Finally in Sec. VIII, we present some discussions and conclude this paper.

II. MODEL AND SIMULATION METHOD

We study the 4D Ising EA SG model, defined by the Hamiltonian

$$H=-\sum_{\langle ij\rangle} J_{ij}S_iS_j-h\sum_i S_i, \tag{1}$$

where the sum runs over pairs of nearest-neighbor sites. Ising variables are defined on a hypercubic lattice with periodic boundary conditions in all directions. The interactions are quenched random variables drawn with equal probability among $\pm J$ with $J>0$. We will use J as the energy unit. The last term in the Hamiltonian represents the Zeeman energy with h being the strength of the external uniform magnetic field. In this representation, the magnetic field h has the dimension of energy so that we will also measure it in the unit of J. In the simulations, we use k_BT/J for the temperature scale and we set the Boltzmann constant $k_B=1$ for simplicity.

It has been well established that a SG phase transition does occur at a finite temperature with strong ordering, namely, a finite amplitude of SG order parameter in the ordered phase. Recent extensive MC studies[25,26] have estimated the critical temperature to be $2.0J$. The critical exponent ν of the diverging coherence length is also obtained as $\nu\sim 0.9-1.0$.[25–27] Another important exponent associated with $T=0$ glassy fixed point is the stiffness exponent θ whose value is also obtained around 0.7 by MC simulation[25] and ground state calculation.[28] We note that the value of $\theta\sim 0.7$ in 4D is significantly larger than that of 3D Ising EA model $\theta_{3D}\sim 0.2$.[29] This fact allows us to analyze the asymptotic behaviors rather easily than 3D case, which is one of our main reasons for investigating the 4D EA model.

The simulation method is a standard single-spin-flip MC method using the two-sublattice dynamics with heat-bath transition probability. We define one Monte Carlo step (MCS) as N spin trials. We also use the multispin coding technique, which simulates 32 different systems independently at the same time on a 32-bit computer. The system sizes studied are $L=8$, 16, 24, and 32 at T_c. Below T_c, we mainly study $L=24$ systems, and $L=32$ in order to check finite-size effects. There is no significant difference between data of $L=24$ and 32 at least within our time window (10^5 MCS).

III. TWO-TIME QUANTITIES

Experimentally, isothermal aging of spin glasses is investigated by observing response of the system to an applied external magnetic field. In the present paper, we study dynamical dc linear magnetic susceptibilities and their conjugate magnetic (spin) autocorrelation function during isothermal aging by Monte Carlo simulations. In the present section, we introduce the two time quantities and summarize some basic properties.

To mimic the experimental protocol of isothermal aging, we consider that the configuration of the system is completely random at time $t=0$ and then start to relax in touch with a heat bath at temperature T which is lower than the critical temperature T_c. Thus cooling rate is infinitely fast.

There are two standard protocols used in dc magnetization measurements. In the so-called zero field cooling (ZFC) procedure, the system first evolves for a waiting time t_w without an applied magnetic field then a small probing magnetic field of strength h is switched on. The growth of the induced magnetization is measured afterwards. In the measurement of the so-called thermoremanent magnetization (TRM), the system evolves under the applied magnetic field of strength h for the waiting time t_w and then the field is cut off. The decay of the magnetization induced during the waiting time is measured afterwards. In our simulations, we measure the linear susceptibility at time $t>t_w$ as

$$\chi(t,t_w)=\frac{1}{N}\frac{\langle M(t)\rangle}{h}, \tag{2}$$

where $M(t)$ is the total magnetization measured at time t with N being the number of spins. The total magnetization is given by sum

$$M(t)=\sum_i S_i(t), \tag{3}$$

where $S_i(t)$ is the Ising spin variable at site i at time t after the quench. Correspondingly, we measure the magnetic (spin) autocorrelation function

$$C(t,t_w)=\frac{1}{N}\langle M(t)M(t_w)\rangle=\frac{1}{N}\sum_i \langle S_i(t)S_i(t_w)\rangle. \quad (4)$$

The last equation holds for our model with no ferromagnetic or antiferromagnetic bias so that the sum of the cross terms of $i\neq j$ vanishes as $1/\sqrt{N}\to 0$ in the thermodynamic limit $N\to\infty$. Furthermore in our Ising model, the spins are normalized $S_i^2=1$ which yields

$$C(t,t)=\frac{1}{N}\sum_i \langle S_i(t)^2\rangle=1 \quad (5)$$

for any t.

In the above equations, $\langle\cdots\rangle$ means to take an average over different realizations of initial conditions, thermal noises and realization of random exchange couplings of the system. However, the above quantities are presumably self-averaging for thermodynamically large systems $N\to\infty$.

If linear response holds, the dynamical linear susceptibilities measured in the ZFC and TRM procedure can be written as

$$\chi_{\rm TRM}(t,t_w)=\int_0^{t_w} dt' R(t,t'), \quad (6)$$

$$\chi_{\rm ZFC}(t,t_w)=\int_{t_w}^{t} dt' R(t,t'), \quad (7)$$

where $R(t,t')$ is the magnetic linear response function. The latter is defined as

$$R(t,t')=\frac{1}{N}\lim_{\delta h\to 0}\frac{\delta\langle M(t)\rangle}{\delta h(t')}, \quad t>t', \quad (8)$$

where $\delta\langle M(t)\rangle$ is the induced magnetization at time t by an infinitesimal probing pulse field $\delta h(t')$ applied only at time $t'(<t)$. From these, it follows that the sum of the two susceptibilities

$$\chi_{\rm ZFC}(t,t_w)+\chi_{\rm TRM}(t,t_w)=\int_0^t dt' R(t,t')=\chi_{\rm ZFC}(t,0) \quad (9)$$

becomes independent of the waiting time t_w and only a function of the total time t elapsed after the temperature quench.[3,30] One can use this sum rule as a criterion to check linearity of measurements.[4,30,31]

Let us briefly discuss the implication of the sum rule (9) combined with the following very mild assumptions. First, the ZFC linear susceptibility $\lim_{t_w\to 0}\chi_{\rm ZFC}(t,t_w)$ increases with t but saturates since it is bounded from above. Let us define in particular the limit

$$\chi_{\rm FC}\equiv\lim_{t\to\infty}\chi_{\rm ZFC}(t,0). \quad (10)$$

We call the latter field cooled (FC) susceptibility because it is more or less similar to what is called FC susceptibility as we discuss below. Second, it is natural to assume weak long term memory[7,8]

$$\lim_{t\to\infty}\chi_{\rm TRM}(t,t_w)=0 \quad (11)$$

for any large but finite t_w. The latter simply means that TRM should relax down to zero for any large but finite waiting time t_w during which the magnetic field is applied. Then we find using above assumptions in the sum rule (9),

$$\lim_{t\to\infty}\chi_{\rm ZFC}(t,t_w)=\lim_{t\to\infty}\chi_{\rm ZFC}(t,0)=\chi_{\rm FC} \quad (12)$$

for any large but finite t_w.

Let us explain why we call Eq. (10) the FC susceptibility. Usually the FC magnetization is measured by cooling down the temperature with a certain cooling rate from above T_c down to a target temperature T below T_c with the magnetic field h being applied. Suppose that it takes time ϵ to cool down the temperature (typically of order 30 sec) and the target temperature is reached at time $t=0$. Then the linear susceptibility measured in this protocol can be expressed as

$$M_{\rm FC}(t)/h=\int_{-\epsilon}^{0} dt' R(t,t')+\chi_{\rm ZFC}(t,0). \quad (13)$$

The above expression is formally valid as long as the linear response holds. Note that the response function in the first term is defined with respect to the particular schedule of the temperature changes. The contribution of the first term decreases with time t because of the weak long term memory property (11). Thus in the limit $t\to\infty$ the susceptibility $M_{\rm FC}(t)/h$ converges to the FC susceptibility of our definition in Eq. (10), $\lim_{t\to\infty}M_{\rm FC}(t)/h=\lim_{t\to\infty}\chi_{\rm ZFC}(t,0)=\chi_{\rm FC}$. The approach to the limit may well be slow. Experimental observations (see, for instance, Fig. 13 of Ref. 3) show that the correction term to the asymptotic limit relaxes slowly but the amplitude is very small such that it can be made much less than 1% of the asymptotic value well within the experimental time window.

In the present paper, we do not discuss the possible effects of finite cooling rates and assume the idealized temperature quench $\epsilon=0$. In this idealized situation, the first term in Eq. (13) is absent and the TRM becomes equivalent to the so-called isothermal remanent magnetization (IRM).

Another interesting limit is to consider $t_w\to\infty$ first with fixed time separation $\tau=t-t_w$. In this limit, one expects to find equilibrium (stationary) response

$$\chi_{\rm eq}(\tau)\equiv\lim_{t_w\to\infty}\chi_{\rm ZFC}(\tau+t_w,t_w), \quad (14)$$

which only depends on the time separation τ. The equilibrium susceptibility $\chi_{\rm EA}$ is defined as

$$\chi_{\rm EA}\equiv\lim_{\tau\to\infty}\chi_{\rm eq}(\tau). \quad (15)$$

The last static susceptibility $\chi_{\rm EA}$ is more or less close to what is called the ZFC magnetization (divided by h).

A very important issue is then whether the two susceptibilities $\chi_{\rm EA}$ and $\chi_{\rm FC}$ are the same or different. As we noted in the Introduction this is intimately related with the fundamental experimental observation in spin-glass systems,[9] namely, $\chi_{\rm FC} > \chi_{\rm ZFC}$. One of the most remarkable finding of the dynamical mean-field theory[8] is that indeed an inequality

$$\chi_{\rm FC} > \chi_{\rm EA} \tag{16}$$

holds with $\chi_{\rm FC}$ defined in Eq. (10) and $\chi_{\rm EA}$ defined in Eq. (15). The difference is due to anomalous contribution of the slowly relaxing, aging part of the response function $R(t,t')$. On the other hand, the conventional droplet theory[13–15] was understood[7] to predict $\chi_{\rm FC}=\chi_{\rm EA}$, i.e., no anomaly. As we explain later in Sec. IV D, our extended droplet theory[12] predicts Eq. (16) with $\chi_{\rm FC}$ being identified with the dynamical susceptibility χ_D associated with the noble dynamical order parameter $q_D(<q_{\rm EA})$ as $k_B T\chi_D = 1-q_D$.

Another important issue is to what extent FDT holds in aging systems. In our present context FDT reads

$$R(t,t') = \frac{1}{k_B T}\partial_{t'} C(t,t') \tag{17}$$

where $C(t,t')$ is the autocorrelation function. It becomes after integration over time $\int_{t_w}^{t} dt' \cdots$,

$$\text{FDT} \quad 1 - C(t,t_w) = k_B T \chi_{\rm ZFC}(t,t_w). \tag{18}$$

Since this *must* hold precisely in equilibrium, the equilibrium limit of ZFC linear susceptibility (14) must be related to that of the spin autocorrelation function as

$$T\chi_{\rm eq}(\tau) = 1 - C_{\rm eq}(\tau), \tag{19}$$

where

$$C_{\rm eq}(\tau) \equiv \lim_{t_w\to\infty} C(\tau + t_w, t_w), \tag{20}$$

is the spin autocorrelation function in the equilibrium. In the static limit $\tau\to\infty$, Eq. (19) becomes the static FDT

$$k_B T\chi_{\rm EA} = 1 - q_{\rm EA}, \tag{21}$$

where $q_{\rm EA}$ is the static EA order parameter defined as

$$q_{\rm EA} = \lim_{\tau\to\infty} C_{\rm eq}(\tau). \tag{22}$$

Except for the ideal equilibrium limit, FDT (18) is not guaranteed in general. However, it was realized recently by Dean, Cugliandolo, and Kurchan that possible amplitude of the violation of the FDT (18)

$$I(t,t_w) \equiv 1 - C(t,t_w) - k_B T\chi_{\rm ZFC}(t,t_w) \tag{23}$$

is bounded from above by the entropy production rate.[32] The bound implies even for very slowly relaxing systems in which entropy production rate becomes small, the FDT (18) should hold between spontaneous thermal fluctuations and linear responses at least for short enough time scales τ.

Let us consider asymptotic limit $t_w\to\infty$ of the two time quantities with fixed value of the autocorrelation function $C = C(\tau + t_w, t_w)$. First let us note that $\lim_{\tau\to\infty} C_{\rm eq}(\tau) = q_{\rm EA}$ implies the time translational invariance (TTI) is strongly broken at $0 < C < q_{\rm EA}$, i.e., the two time quantities cannot be a function of only the time separation in this regime. Concerning the integral FDT violation (23), it becomes a function of C, i.e., $\lim_{t_w\to\infty} I(t,t_w) = I(C)$. In conventional cases $I(q_{\rm EA} < C < 1) = 0$ while $I(0 < C < q_{\rm EA}) > 0$ being a nontrivial function of C by the dynamical MFT (Refs. 8 and 33) and $I(0 < C < q_{\rm EA}) = q_{\rm EA} - C$ in usual coarsening systems.[34–36] On the other hand, our scenario[12] suggests $I(q_D < C < 1) = 0$ and $I(0 < C < q_D) = q_D - C$. Here q_D is the new dynamical order parameter which is smaller than $q_{\rm EA}$. Thus the breaking points of TTI and FDT take place separately at $q_{\rm EA}$ and q_D, respectively, in our scenario while both of them take place simultaneously at $q_{\rm EA}$ in the dynamical MFT and usual coarsening systems.[34–36]

IV. THEORETICAL BACKGROUND

In this section we discuss our extended droplet theory sketched in Ref. 12 concerning isothermal aging which will be our basis to analyze the data of Monte Carlo simulations in later sections. As we noted in the introduction, we pay a special attention to the idea of so-called effective stiffness of droplet excitations in the presence of domain walls which are present as extended defects during isothermal aging. For clarity, we will try to present this section in a self-contained fashion including summaries of the results of the original droplet theory[14,15] which are almost fully included in our scenario. To simplify notations, we consider systems of N Ising spins $S_i = \pm 1$ $(i = 1, \ldots, N)$ in a d-dimensional space coupled by short-ranged interactions of energy scale J with random signs with no ferromagnetic or antiferromagnetic bias.

A. Basics

Let us recall briefly the starting point of the droplet theory.[14] It assumes that thermodynamic states of (Ising) spin-glass phases consist of a pair of pure states of an infinite system which are related by global spin inversion. At low but finite temperature in the spin-glass phase, an equilibrium state can be considered as made of a ground state, say Γ or its global spin inversion $\overline{\Gamma}$, plus thermally activated droplet excitations of various sizes taking place on top of Γ. In simple systems such as ferromagnets droplet excitations exist but play a rather limited role.[34] An essential finding of the original droplet theory[13,14] is that the temperature is *dangerously irrelevant* in spin-glass phases because of strong impacts of thermally activated droplets.

A droplet at a given length scale L is supposed to be a compact cluster of spins with a volume L^d with d being the dimension of the space and a surface volume L^{d_f} with d_f being the (fractal) surface dimension. The typical value of its excitation gap $F_L^{\rm typ}$ with respect to the ground state is supposed to scales as

$$F_L^{\rm typ} \sim \Upsilon (L/L_0)^{\theta}, \tag{24}$$

where the exponent $\theta>0$ is the stiffness exponent, Υ is the stiffness constant, and L_0 is a microscopic length scale. The excitation gap is, however, broadly distributed with the typical value given above. The probability distribution of the free-energy gap is expected to follow a universal scaling form

$$\rho(F_L)dF_L=\tilde{\rho}(F_L/F_L^{\rm typ})dF_L/F_L^{\rm typ} \tag{25}$$

with nonvanishing amplitude at the origin

$$\tilde{\rho}(0)>0 \tag{26}$$

which allows marginal droplets. This property $\tilde{\rho}(0)>0$ allows dangerously active droplets which will respond to arbitrarily weak perturbations so that they play extremely important roles as the Goldstone modes: they dominate spontaneous thermal fluctuations and linear responses.

Dynamically, the excitation of such a cluster of spins is supposed to happen only by thermal activated process. The typical value of free-energy barrier $B_L^{\rm typ}$ to flip the cluster of spins is supposed to scale as

$$B_L^{\rm typ}\sim\Delta(L/L_0)^{\psi}, \tag{27}$$

where Δ is a characteristic free-energy scale of the barriers. The Arrhenius law implies that a droplet of length scale $L(t)$,

$$L(t)\sim\left(\frac{k_BT}{\Delta}\ln(t/\tau_0)\right)^{1/\psi}, \tag{28}$$

can be activated within a time scale of t. Here τ_0 is a certain unit time scale for the activated processes. Let us call this time-dependent length scale as the dynamical length scale.

B. Crossover from critical to low temperature regime

In practice, it is necessary to take into account of critical fluctuations near T_c. Even at $T<T_c$, the length scales shorter than the coherence length of the critical fluctuation

$$\xi_-\sim L_0|1-T/T_c|^{-\nu} \tag{29}$$

should be dominated by critical fluctuations. Asymptotic low temperature properties should appear only at larger length scales.

Correspondingly, we expect two typical stages in the dynamical length scale $L(t)$ as shown in Fig. 1. One is a critical dynamics associated with critical slowing down in time range $\tau_0(T)\gg t\gg t_0$, where $L(t)$ follows a power law with the dynamical critical exponent z,

$$L(t)=l_0(t/t_0)^{1/z}. \tag{30}$$

Here l_0 is a microscopic length scale which is of order 1 lattice distance in EA models and t_0 is a microscopic time scale which is typically $t_0\sim10^{-12}-10^{-13}$ (sec) in real spin systems while it is 1 Monte Carlo Step (MCS) in usual heat-bath Monte Carlo simulations. This formula means that even at $T<T_c$, $L(t)$ behaves like the critical power law at short time-length scales. On the other hand, the intrinsic low-temperature dynamics associated with the $T=0$ glassy fixed point (28) should occur only at larger time scales beyond a certain crossover time $t\gg\tau_0(T)$.

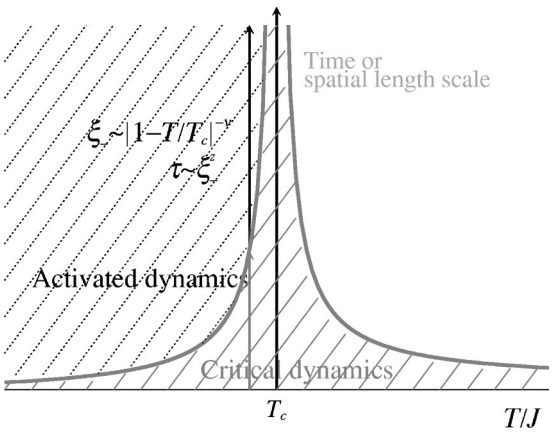

FIG. 1. Schematic picture of length scale.

The crossover length $L_0(T)$ would be determined by a comparison between free-energy barrier and thermal energy

$$k_BT\sim\Delta(T)[L_0(T)/l_0]^{\psi}, \tag{31}$$

where the characteristic free-energy scale $\Delta(T)$ behaves as $\Delta(T)=J|1-T/T_c|^{\psi\nu}$ near T_c.[15] It leads to the temperature dependence of $L_0(T)$,

$$L_0(T)=l_0(T/J)^{1/\psi}|1-T/T_c|^{-\nu}, \tag{32}$$

which is essentially equivalent to Eq. (29). The corresponding crossover time $\tau_0(T)$ is given by

$$\tau_0(T)=t_0[L_0(T)/l_0]^z. \tag{33}$$

We obtain the singular part of the crossover time at T, $\tau_0(T)\sim|1-T/T_c|^{-z\nu}$, as expected from a critical scaling theory. Consequently, the scaling formula of the growth law which describes the whole crossover from the critical dynamics at $t\ll\tau_0(T)$ and the activated dynamics at $t\gg\tau_0(T)$ is given by

$$L(t)/L_0(T)=\tilde{L}[t/\tau_0(T)], \tag{34}$$

where

$$\tilde{L}(x)\sim\begin{cases}x^{1/z} & (x\ll1),\\ \ln^{1/\psi}(x) & (x\gg1).\end{cases} \tag{35}$$

One should note that the crossover could be very gradual and functional form of the intermediate regime (which will dominate realistic time ranges in simulations and experiments) can have very complicated expression which is not obvious. This crossover in the growth law of the dynamical length scale is numerically examined in Sec. V.

The importance of the crossover from critical to low temperature behavior has been pointed out by Bokil *et al.*[37] concerning some static properties of low-temperature SG phase. Let us note that the above analysis of the crossover from the critical to activated dynamics is a direct (dynamical) analogue of the analysis of defect free-energy in 4D EA model[25]

by one of us (K.H.). In the latter study, the defect free-energy was found to become a universal constant in the limit $L \ll \xi_-$ and grows as $\Upsilon(T)(L/L_0)^\theta$ and $\Upsilon(T) \sim J|1-T/T_c|^{\theta\nu}$ with $\theta=0.82$, $\nu=0.93$ at $L \gg \xi_-$.

C. Domain growth

During isothermal aging up to a time t after quench, domains with the mean size $L(t)$ separating different pure states grow up by coarsening domain walls of smaller length scales. The droplet theory proposed scaling properties of time-dependent physical quantities in terms of time-dependent mean domain size $L(t)$. We discuss the scaling by $L(t)$ of one-time quantities with time elapse after the quench, which examine later by MC simulations. One example is time development of energy per spin defined by

$$e(t) = -\frac{1}{N}\sum_{\langle ij\rangle} \langle J_{ij} S_i(t) S_j(t)\rangle. \tag{36}$$

Relaxation of the energy per spin is expected to be due to relaxation of excessive energy associated with domain walls. Thus it is expected to decrease as[22]

$$e(t) - e_{\rm eq} = \Upsilon' \left(\frac{L(t)}{l_0}\right)^{\theta-d}, \tag{37}$$

where Υ' is a temperature-dependent parameter.

Another interesting one-time quantity is domain-wall density $\rho_s(t)$ in which the morphology of the domain with the fractal surface dimension $d_f \geqslant d-1$ appears. In coarsening dynamics the density decreases with time during isothermal aging. In simple systems such as a ferromagnet where the domain wall becomes flat at sufficiently low temperature, the density of domain wall is proportional to the inverse of the mean size $1/L(t)$. However, it could be rough with the fractal dimension in spin glasses because of the disorder and frustration so that we expect

$$\rho_s(t) \sim \left(\frac{L(t)}{l_0}\right)^{d_f-d}. \tag{38}$$

In MC simulations, two replicas with identical interaction bonds are updated independently and the domain-wall density is calculated as[21]

$$\rho_s(t) = \frac{1}{2}\left(1 - \frac{1}{N_B}\sum_{\langle ij\rangle} \sigma_i^{(\alpha)}(t)\sigma_j^{(\alpha)}(t)\sigma_i^{(\beta)}(t)\sigma_j^{(\beta)}(t)\right), \tag{39}$$

where N_B is the number of bonds and the suffixes α and β denote replica indices. Here, following Ref. 21 we take short time average of each spin as

$$\sigma_i^{(\alpha)}(t) = \mathrm{sgn}\left(\sum_{\tau=t/2}^{t} S_i^{(\alpha)}(\tau)\right). \tag{40}$$

This procedure in Eq. (40) means that smaller fluctuations associated with small droplets are eliminated and the coarsening domain walls are emphasized. Without taking such average over time, the density is similar to so-called link overlap function, which does not vanish in the long time limit.

D. Domain walls and soft droplets

Following Ref. 15, the whole process of isothermal aging may be divided into *epoch*s such that the typical separation between domain walls (hereafter simply denoted as domain size) $L_0, aL_0, a^2L_0, \ldots, a^nL_0, \ldots$ where $a>1$. At each epoch, droplets of various sizes up to that of the domain size can be thermally activated or polarized by the magnetic field. The two time quantities we introduced in Sec. III, namely, the autocorrelation function $C(\tau+t_w, t_w)$ defined in Eq. (4) and the linear susceptibility $\chi(\tau+t_w, t_w)$ defined in Eq. (2) probe such thermal fluctuations and linear responses of droplets smaller than the size of the domain if the time separation is limited such that $L(\tau) \leqslant L(t_w)$.

In a previous work,[12] we extended the idea of Fisher and Huse[15] who noticed that droplet excitations can be softened in the presence of a frozen-in defect or domain wall compared with ideal equilibrium with no extended defects. This is because droplets which touch the defects can reduce the excitation gap compared with those in equilibrium. This effect will have very important impacts on the two time quantities.

Let us consider a system with a frozen-in defect of size R: a large droplet of size R is flipped with respect to Γ, which is a ground state of an infinite system, and then it is frozen. The typical free-energy gap $F_{L,R}^{\rm typ}$ of a smaller droplet of size L in the interior of the frozen-in defect is expected to scale as

$$F_{L,R}^{\rm typ} = \Upsilon_{\rm eff}[L/R](L/L_0)^\theta, \quad L<R \tag{41}$$

with $\Upsilon_{\rm eff}[L/R]$ being an effective stiffness which is only a function of the ratio $y=L/R$.

For $y \ll 1$, $\Upsilon_{\rm eff}[y]$ will decrease with y as[15]

$$\Upsilon_{\rm eff}[y]/\Upsilon = 1 - c_v y^{d-\theta} \quad \text{for} \quad y \ll 1. \tag{42}$$

Here Υ is the original stiffness constant $\Upsilon = \Upsilon_{\rm eff}(0)$. A basic conjecture, on which our new scenario based, is that at the other limit $y \sim 1$ the effective stiffness vanishes as

$$\Upsilon_{\rm eff}[y]/\Upsilon \sim (1-y)^\alpha, \quad y \sim 1 \tag{43}$$

with $0<\alpha<1$ being an unknown exponent, and that the lower bound for $F_{L,R}^{\rm typ}$ should be of order J, say F_0.

We assume that the probability distribution of the free-energy gap $F_{L,R}$ is broad and obey the same functional form as Eq. (25) where $F_L^{\rm typ}$ should be replaced by $F_{L,R}^{\rm typ}$. Then the scaling form of the distribution of the gap (25) and nonzero amplitude of gapless droplets $\tilde{\rho}(0)>0$ (26) implies that the probability that a gap is smaller than a certain threshold $\delta U (\ll F_L^{\rm typ})$ scales as

$$\mathrm{Prob}(F_{L,R} < \delta U) \sim \tilde{\rho}(0)\,\delta U / F_{L,R}^{\rm typ}. \tag{44}$$

Since the probability is *linear* with δU, these active droplet are dangerously irrelevant:[13–15] arbitrary small perturbation δU may trigger a droplet excitation.

1. Two length quantities

To explain the consequence of our conjecture above introduced, let us consider thermal fluctuations and magnetic linear responses of droplet excitations of size L enclosed in a compact region made by a frozen-in defect at scale R which has $N_d \propto (R/L_0)^d$ spins. To this end, let us construct a toy droplet model[14] defined on logarithmically separated shells of length scales $L_k/L_0 = a^k < R/L_0$ with $a>1$ and $0 \leqslant k \leqslant n_2 \leqslant n_1$ where $R/L_0 = a^{n_1}$ and $L_m/L_0 = a^{n_2}$. For each shell an *optimal* droplet is assigned whose free-energy gap is minimized within the shell. Then $F^{\rm typ}_{L,R}$ will be of order F_0 at the shell $k=n_1$ so that we have

$$\tilde{F}^{\rm typ}_{L,R} = F^{\rm typ}_{L,R}(1-\delta_{k,n_1}) + F_0 \delta_{k,n_1}. \tag{45}$$

For simplicity, droplets at different scales are assumed to be independent from each other.

At the shell $L/L_0 = a^k$, the system is decomposed into compact cells of volume L^d such that each cells represents a droplet of size L. The number density of droplets per spin associated with the shell scales as

$$N_d \left(\frac{L}{L_0}\right)^{-d} \ln a. \tag{46}$$

Each droplet excitation will induce a random change of the magnetization of order

$$M_L \sim m \sqrt{(L/L_0)^d}, \tag{47}$$

where m is the average magnetic moment within a volume of L_0.

The thermal fluctuation can be measured by an order parameter

$$q = \overline{N_d^{-1} \sum_i \langle S_i \rangle^2}, \tag{48}$$

where the sum runs over sites in the interior of the frozen-in defect. Here we have put the overline which means to take average over different realization of the randomness. In the absence of any droplet excitations, $q=1$ holds due to the normalization of the Ising spins. A spontaneous thermal fluctuation of a droplet will take place if its excitation gap happens to be smaller than the thermal energy $k_B T$. The probability of the latter is found to be proportional to $\tilde{\rho}(0) k_B T / F^{\rm typ}_{L,R}$ due to Eq. (44). So the reduction from 1 due to a droplet excitation at scale L is of order $M_L^2 \tilde{\rho}(0) \times (k_B T / F^{\rm typ}_{L,R})$. Then the reduction of the spin autocorrelation by droplet excitations at scale L is estimated as

$$\delta q_L \sim M_L^2 \tilde{\rho}(0) \frac{k_B T}{F^{\rm typ}_L} \left(\frac{L}{L_0}\right)^{-d} \ln a, \tag{49}$$

where the last factor is due to the number of droplets per spin given in Eq. (46).

The magnetic linear response by weak external magnetic field h is measured by a linear susceptibility

$$\chi = \lim_{h \to 0} \overline{N_d^{-1} \sum_i \langle S_i \rangle_h / h}, \tag{50}$$

where $\Sigma_i \langle S_i \rangle_h$ is the induced magnetization by the field. Since a droplet excitation can induce a magnetization of order M_L given in Eq. (47) with random signs, it can gain a Zeeman energy of order $\delta U_L \sim M_L \delta h$ by responding to the field. The probability that the droplet excitation takes place is then proportional to the probability that the gain by the Zeeman energy is larger than the excitation gap of the droplet which can be found using Eq. (44). Then the expectation value of the magnetic moment induced by droplet excitations at scale L is estimated as

$$h \delta \chi_L \sim M_L \tilde{\rho}(0) \frac{h M_L}{F^{\rm typ}_L} \left(\frac{L}{L_0}\right)^{-d} \ln a. \tag{51}$$

Now summing over contributions at different length scales $0<k<n_2$, we obtain the total reduction of the order parameter from 1 and the linear susceptibility as using Eqs. (45), (49), and (51) by

$$\begin{aligned} 1 - q(L_m, R) &= k_B T \chi(L_m, R) \\ &= \tilde{\rho}(0) m^2 \sum_{k=0}^{n_2} \frac{k_B T}{F^{\rm typ}_{L,R}(1-\delta_{k,n_1}) + F_0 \delta_{k,n_1}} \\ &= \tilde{\rho}(0) m^2 k_B T \int_{L_0}^{L_m} \frac{dL}{L} \left[\frac{1 - \Delta_a[\ln(L/R)]}{F^{\rm typ}_{L,R}} \right. \\ &\quad \left. + \frac{\Delta_a[\ln(L/R)]}{F_0} \right]. \end{aligned} \tag{52}$$

In the last equation, the sum $\Sigma_{k=0}^{n_2}$ is replaced by an integral $\int_{L_0}^{L_m} dL/L$ and $\Delta_a(z)$ is a pseudo-δ-function of width $\ln a$.[38] Note that FDT is satisfied between Eqs. (49) and (51).

In the following let us call the two length quantities $q(L,R)$ and $\chi(L,R)$ as the generalized order parameter and the generalized linear susceptibility, respectively. We will associate these two length quantities with the two time quantities measured in aging experiments.

2. Edwards-Anderson order parameter

For clarity, let us consider the *equilibrium limit* where there is no extended defects which can be realized by taking $R \to \infty$ first. In the latter limit we recover the result of the original droplet theory[14]

$$\lim_{R \to \infty} q(L,R) = q_{\rm EA} + c \frac{\tilde{\rho}(0) m^2 k_B T}{\Upsilon (L/L_0)^\theta}, \tag{53}$$

with

$$c = \int_1^\infty dy\, y^{-1-\theta}. \tag{54}$$

and the Edwards-Anderson (EA) order parameter defined in Eq. (22) evaluated as

$$q_{\rm EA}=\lim_{L\to\infty}\lim_{R\to\infty} q(L,R)=1-c\tilde{\rho}(0)m^2\frac{k_BT}{\Upsilon}. \tag{55}$$

The associated *equilibrium* susceptibility $\chi_{\rm EA}$ is defined as Eq. (21) $k_BT\chi_{\rm EA}\equiv 1-q_{\rm EA}$. The above expressions become useful when we consider equilibrium dynamics.

3. Dynamical order parameter

It is useful to consider asymptotic behavior at large sizes $R/L_0\gg 1$ with the ratio $x=L_m/R$ being fixed. We obtain for $0<x\leqslant 1$,

$$q(xR,R)=q_{\rm EA}+\frac{\tilde{\rho}(0)m^2k_BT}{\Upsilon(R/L_0)^\theta}A(x)-\frac{\tilde{\rho}(0)m^2k_BT}{F_0}\Theta_a(\ln x) \tag{56}$$

with $\Theta_a(z)$ being a pseudo-step-function of width $\ln a$ (Ref. 38) and

$$A(x)=\int_x^\infty dy y^{-1-\theta}-\int_0^x dy y^{-1-\theta} \times\{\Upsilon/\Upsilon_{\rm eff}[y][1-\Delta_a(\ln y)]-1\}. \tag{57}$$

Note that the second integral converges because of Eq. (42) and the inequality $\theta<(d-1)/2$.[14] Thus as far as $0<x<1$, the order parameter converges to the *equilibrium* EA order parameter $q_{\rm EA}$ evaluated in Eq. (55).

In the intriguing case $x\sim 1$, $A(x)$ will remain finite as far as $0<\alpha<1$. At $x\sim 1$ the last term of Eq. (56), which is due to the anomalously soft droplets, contributes and we obtain

$$q(R,R)=q_D+A(1)\frac{\tilde{\rho}(0)m^2k_BT}{\Upsilon(R/L_0)^\theta}, \tag{58}$$

where we have defined the dynamical order parameter

$$q_D\equiv\lim_{R\to\infty} q(R,R)=q_{\rm EA}-\tilde{\rho}(0)m^2\frac{k_BT}{F_0}. \tag{59}$$

Naturally, we can define the associated dynamical linear susceptibility χ_D as

$$k_BT\chi_D\equiv 1-q_D. \tag{60}$$

The above results imply

$$q_D<q_{\rm EA} \tag{61}$$

and

$$\chi_D>\chi_{\rm EA}. \tag{62}$$

As we discuss below q_D and χ_D play significantly important roles in the dynamical observables of aging. We will see that the field cooled susceptibility $\chi_{\rm FC}$ defined in Eq. (10) is equal to the dynamical susceptibility χ_D defined above. Thus the inequality (62) implies the anticipated inequality $\chi_{\rm FC}>\chi_{\rm EA}$ given in Eq. (16).

4. Two-time and two-length quantities

We can now associate the two length quantities discussed above with the two time quantities for short time separations $L(\tau)\leqslant L(t_w)$. In the latter regime, the autocorrelation function $C(\tau+t_w,t_w)$ and the ZFC linear susceptibility $\chi_{\rm ZFC}(\tau+t_w,t_w)$ measure, respectively, thermal fluctuations and linear responses of droplets smaller than the size of the domain $L(t_w)$.

The autocorrelation function at a given time separation τ probes thermal fluctuations of droplets as large as $L(\tau)$ in the presence of domain walls of size $R(t_w)$ so that we expect

$$C(\tau+t_w,t_w)=q[L(\tau),L(t_w)], \tag{63}$$

where $q(L,L')$ is the generalized order parameter given in Eq. (52). Similarly, the ZFC susceptibility probes the polarization of droplets as large as $L(\tau)$ in the presence of domain walls of size $R(t_w)$ we expect

$$k_BT\chi_{\rm ZFC}(\tau+t_w,t_w)=k_BT\chi[L(\tau),L(t_w)] =1-C(\tau+t_w,t_w), \tag{64}$$

where $\chi(L,L')$ is the generalized susceptibility given in Eq. (52).

Let us note that the generalized order parameter $q(L,L')$ and the generalized susceptibility $\chi(L,L')$ are defined via disorder averaging of many different realization of small systems of size L'. Here it is important to recall that at any finite time, a macroscopic system will contain macroscopic number of domains no matter how large their size $L'=L(t_w)$ is. Thus we can safely evaluate these two time quantities, which are macroscopic quantities, by the disorder-averaged two-length quantities.

Let us emphasize that the FDT (18) is satisfied while time translational invariance (TTI) is broken in the above two length/time quantities for $L(\tau)\leqslant L(t_w)$. The latter is due to the fact that the autocorrelation function and the susceptibility depends on two length/time, i.e., not only $L(\tau)$ but also on $L(t_w)$. For larger time separations $L(\tau)>L(t_w)$, we take into account decay of memory due to coarsening of domain walls following the original droplet theory.[15]

E. Scaling properties of two-time quantities

Using the results of the previous section, we now discuss scaling properties of the two time quantities at different regimes in detail. Basically we expect three distinct regimes (i) quasiequilibrium regime $L(\tau)<L(t_w)$, (ii) crossover regime $L(\tau)\sim L(t_w)$, and (iii) aging regime $L(\tau)>L(t_w)$. In the following we first consider the ideal equilibrium limit for clarity and then the three regimes subsequently.

1. Equilibrium limit

Let us consider first the equilibrium limits of the autocorrelation function and the ZFC susceptibility which are obtained by taking the limit $L(t_w)\to\infty$ with fixed $L(\tau)$ in Eqs. (52), (63), and (64). From Sec. IV D 2 one immediately finds[15]

$$C_{\rm eq}(\tau)=q_{\rm EA}+c\tilde{\rho}(0)m^2(k_BT/\Upsilon)[L(\tau)/L_0]^{-\theta} \quad (65)$$

and

$$\chi_{\rm eq}(\tau)\equiv\lim_{t_w\to\infty}\chi_{\rm ZFC}(\tau+t_w,t_w)=\chi_{\rm EA}-c\frac{\tilde{\rho}(0)m^2}{\Upsilon[L(\tau)/L_0]^{\theta}}. \quad (66)$$

In Eq. (65) $q_{\rm EA}$ is the EA order parameter defined in Eq. (22) and evaluated in Eq. (55). The numerical constant c is given in Eq. (54). Correspondingly $\chi_{\rm EA}$ is the equilibrium susceptibility related to $q_{\rm EA}$ as $k_BT\chi_{\rm EA}=1-q_{\rm EA}$ as in Eq. (21).

2. Quasiequilibrium regime

Now we discuss the quasi-equilibrium regime $L(\tau)<L(t_w)$. The autocorrelation function and ZFC linear susceptibility can be evaluated using Eqs. (52), (63), and (64). For simplicity, here we assume to stay deep in the quasiequilibrium regime $L(\tau)\ll L(t_w)$. Then using the scaling property of the effective stiffness (42), one obtains[23]

$$C(t=\tau+t_w,t_w)=C_{\rm eq}(\tau) - c'\tilde{\rho}(0)m^2\frac{k_BT}{\Upsilon[L(\tau)/L_0]^{\theta}}\left(\frac{L(\tau)}{L(t_w)}\right)^{d-\theta} + \cdots, \quad (67)$$

with $C_{\rm eq}(\tau)$ being the equilibrium part given in Eq. (65) and $c'=c_v\int_0^1 dy y^{2[(d-1/2)-\theta]}$. The second term is the weak nonequilibrium correction term due to the weak softening of small droplets which gives rise to some weak waiting time dependences.

The above formula combined with the formula for the equilibrium part (65) yields a systematic extrapolation scheme to determine the EA order parameter $q_{\rm EA}$. Such an extrapolation was already demonstrated in our previous paper.[17] In Sec. VII C, we perform such an analysis numerically.

Similarly, the ZFC susceptibility $\chi_{\rm ZFC}(\tau+t_w,t_w)$ is evaluated as

$$k_BT\chi_{\rm ZFC}(t=\tau+t_w,t_w)=k_BT\chi_{\rm eq}(\tau)+c'\tilde{\rho}(0)m^2 \times\frac{k_BT}{\Upsilon[L(\tau)/L_0]^{\theta}}\left(\frac{L(\tau)}{L(t_w)}\right)^{d-\theta}+\cdots \quad (68)$$

with $\chi_{\rm eq}(\tau)$ being the equilibrium part given in Eq. (66) and $\chi_{\rm EA}$ is the equilibrium susceptibility.

The quasiequilibrium regime is most relevant for the measurements of the relaxation of ac susceptibilities during isothermal aging. Recently a related scaling analysis was performed in an experiment.[19] Let us note that previous experimental analysis of spontaneous thermal fluctuation of the magnetization and ac susceptibility have already confirmed that FDT holds for quasiequilibrium regime while nonstationarity is observed clearly.[4,39,40]

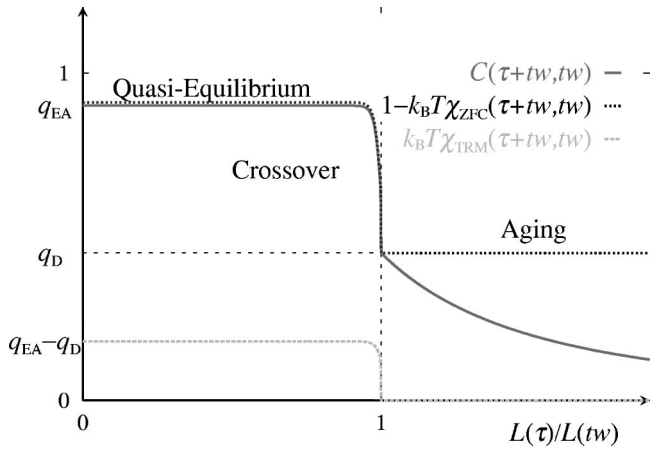

FIG. 2. Different asymptotic regimes of the two-time quantities. See text for details.

3. Crossover regime

Next let us consider the crossover regime $L(\tau)\sim L(t_w)$. Here we have to consider also the contribution of anomalously soft droplets of sizes as large as that of the domain.

From Eq. (58) the spin autocorrelation function is obtained immediately as

$$C(\tau+t_w,t_w)|_{L(\tau)/L(t_w)\sim 1} \sim q_D+\tilde{\rho}(0)m^2A(1)\frac{k_BT}{\Upsilon[L(t_w)/L_0]^{\theta}}, \quad (69)$$

where q_D is the dynamical order parameter defined in Eq. (59). Similarly the ZFC susceptibility is obtained as

$$k_BT\chi_{\rm ZFC}(t_w+t_w,t_w)|_{L(\tau)/L(t_w)} {}_{\sim 1}\sim k_BT\chi_D-\tilde{\rho}(0)m^2A(1)\frac{k_BT}{\Upsilon[L(t_w)/L_0]^{\theta}}, \quad (70)$$

where χ_D is the dynamical susceptibility defined in Eq. (60).

As we discuss in Sec. IV E 6, the change from the quasiequilibrium regime and the crossover regime becomes very abrupt as function of $x=L(\tau)/L(t_w)$ in the asymptotic limit $L(t_w)\to\infty$ (see Fig. 2). This feature deserves to be studied in simulations and experiments. A convenient measure is the modified relaxation rate function $S_{\rm mod}(x,t_w)$ we introduce in Eq. (91).

4. Aging regime: autocorrelation function

Let us now consider aging regime $L(t)\sim L(\tau)>L(t_w)$ where we need to consider growth of the domains explicitly. For simplicity, we used the notion of *epochs* mentioned previously.[15] The nth epoch spans logarithmically separated time scales between t_{n-1} and t_n such that $L(t_{n-1})=a^{n-1}L_0$ and $L(t_n)=a^nL_0$ with $a>1$. At each epoch some of the smaller domains are eliminated so that domain walls are coarsened. Thus a given site may or may not belong to the same domain (Γ or $\bar{\Gamma}$) at two different epochs. The probability $P_s(R_1,R_2)$ that a given site belongs to the same do-

main at the two different epochs characterized by the sizes of the domains R_1 and R_2 presumably becomes a function of the ratio of the size of the domains, i.e.,

$$P_s(R_1,R_2)=P_s\left(\frac{R_1}{R_2}\right) \tag{71}$$

reflecting the self-similar nature of the domain growth process.[15,35] This function describes the slow decay of memory by the domain growth and plays the central role in the following.

For simplicity, let us neglect thermally active droplet excitations in the interior of the domains and consider only the domain growth itself for the moment. Then the autocorrelation function between two epochs such that size of domains are $R_1=L(t)$ and $R_2=L(t_w)$ becomes

$$C(t=\tau+t_w,t_w)=\tilde{C}\left(\frac{L(t)}{L(t_w)}\right) \tag{72}$$

with

$$\tilde{C}(x)=2P_s(x)-1. \tag{73}$$

In the limit $x\to 1^+$, the scaling function should converge as

$$\lim_{x\to 1^+}\tilde{C}(x)=1, \tag{74}$$

because the normalization of the Ising spins. In the other limit, the scaling function is expected to behave asymptotically as

$$\tilde{C}(x)\sim x^{-\lambda} \quad (x\gg 1) \tag{75}$$

with λ being a nonequilibrium exponent[15,35]

$$d/2<\lambda<d. \tag{76}$$

By taking into account thermally active droplet excitations, we expect the scaling form of the spin autocorrelation function as

$$C(t,t_w)\sim q_D\tilde{C}\left(\frac{L(t)}{L(t_w)}\right), \tag{77}$$

where q_D is the dynamical order parameter introduced in Eq. (59). Note that in usual coarsening process,[35,36,41] the amplitude is given by EA order parameter $q_{\rm EA}$ which was also assumed in the original droplet theory.[15] However, we expect the dynamical order parameter q_D is more natural because of the anomalously soft droplets which are as large as domains. The above scaling form (77) should be manifested in the asymptotic limit $L(t_w)\to\infty$ with the ratio $x=L(t)/L(t_w)$ fixed to a certain value larger than 1. Note that the normalization (74) allows matching with the crossover regime discussed in the previous section in the asymptotic limit $L(t_w)\to\infty$.

At finite time scales, we expect some correction terms because of the following reasons. First let us recall that the asymptotic amplitude of the order parameter is attained only by integrating out contributions of droplet excitations up to infinitely large ones. At finite length scales, the amplitude of the order parameter should be larger than q_D due to the algebraic correction term such as the second term in Eq. (58) or (69). Then the factor q_D in the scaling form (77) should be replaced by some time-dependent factor at finite time scales. Second, we also expect some additive correction terms since with some probability there will be some region where domain walls do not pass through so that the dynamics due to droplets in the interior of the domains continues. Such quasiequilibrium corrections will be additive as considered in dynamical MFT.[8] However, we do not know how to collaborate both the multiplicative and additive correction terms simultaneously and we will leave the problem of correction terms for the autocorrelation function in the aging regime for future studies.

5. Aging regime: linear susceptibilities

Finally let us consider the linear response to magnetic field during the domain growth (aging). Suppose that magnetic field h is applied only during a certain *epoch* where the size of the domain is $L_n/L_0=a^n$ with n being a certain positive integer. Then let us consider the magnetization $\delta M_n(t)$ measured at some time $t>t_{n-1}$ during and after the epoch,

$$\delta M_n(t)=h\int_{t_{n-1}}^{\min(t,t_n)}dt'R(t,t'), \tag{78}$$

where $R(t,t')$ is the response function defined in Eq. (8).

During the epoch, droplets over the length scales from L_0 up to $L(\tau=t-t_{n-1})$ can be polarized by the field. Importantly the size of the domain can be considered as frozen in time to the value L_n during this epoch so that the linear response is the same as that in the quasiequilibrium/crossover regimes. Thus the magnetization measured within the same epoch will be

$$\delta M_n(t)\sim h\chi[L(\tau),L_n]$$
$$\sim h\tilde{\rho}(0)\int_{L_0}^{L(\tau)}\frac{dL}{L}\frac{m^2}{F^{\rm typ}_{L,L_n}} \quad \text{for} \quad t_{n-1}<t<t_n \tag{79}$$

where we used the generalized susceptibility given in Eq. (52). This part due to the droplets satisfies the FDT (18).

When the field is cut off at time t_n, depolarization of the droplets will start. Let us now follow the argument of Fisher and Huse,[15] and first consider a certain early stage of the $(n+1)$-th epoch, say up to time t_n^+ slightly after t_n, such that further domain growth still does not proceed appreciably. Note that the switching off of the field is equivalent to adding additional field of the opposite sign $-h$. The latter will induce additional negative magnetization whose amplitude grow similar to Eq. (79) with τ being understood as the time after the field change. Up to the time t_n^+ most of the magnetizations will be canceled. However, some residual magnetization of order

$$\delta M_n(t_n^+) \sim c'' \tilde{\rho}(0) \frac{hm^2}{\Upsilon (L_n/L_0)^\theta} \tag{80}$$

may be left behind. Here c'' is a certain numerical constant. As domain growth proceeds further, the residual magnetization will remain only if the domain to which the polarized droplet belongs is not eliminated. Then the remanent magnetization will decay by the further domain growth as

$$\delta M_n(t) \sim \delta M_n(t_n^+) \left[2P_s\left(\frac{L(t)}{L_n} \right) - 1 \right]$$

$$\sim c'' \tilde{\rho}(0) \frac{hm^2}{\Upsilon (L_n/L_0)^\theta} \tilde{C}\left(\frac{L(t)}{L_n} \right) \quad \text{for} \quad t \gg t_n . \tag{81}$$

Here $\tilde{C}[L(t)/L]$ is related to the probability $P_s[L(t)/L]$ that a given site belongs to the same domain at the two different epochs L_n and $L(t)(>L_n)$ as given in Eq. (73). This is the aging part of the response which violates the FDT (18) strongly.

Combining the above results we can now evaluate the ZFC and TRM susceptibilities defined in Eqs. (7) and (6) by summing over the responses at different epochs given by Eqs. (79) and (81). Suppose that the observation time t belongs to the nth epoch and the waiting time t_w belongs to the mth epoch such that $m<n$. Then the ZFC susceptibility is obtained as

$$\chi_{\rm ZFC}(t,t_w) = \int_{t_w}^{t} dt' R(t,t')$$

$$= \frac{1}{h} \sum_{k=m}^{n} \delta M_k(t) \sim \chi[L(\tau), L(t)]$$

$$+ c'' \int_{L(t_w)}^{L(t)} \frac{dL}{L} \frac{\tilde{\rho}(0) m^2}{\Upsilon (L/L_0)^\theta} \tilde{C}\left(\frac{L(t)}{L} \right). \tag{82}$$

The first term in the last equation is the response of droplets (79) during the last epoch where the observation is being done and second term is the aging part (81) due to the remanence of the response made at previous epochs. Note that the expression is valid also for the quasiequilibrium and crossover regimes because there $L(t) \sim L(t_w)$ holds and the second term is absent so that the expression becomes the same as Eq. (64).

In the special case of $t_w = 0$, the above result becomes

$$\chi_{\rm ZFC}(t,0) \sim \chi[L(t),L(t)] + c'' \int_{L_0}^{L(t)} \frac{dL}{L} \frac{\tilde{\rho}(0) m^2}{\Upsilon (L/L_0)^\theta} \tilde{C}\left(\frac{L(t)}{L} \right)$$

$$\sim \chi_D - c''' \frac{\tilde{\rho}(0) m^2}{\Upsilon [L(t)/L_0]^\theta}, \tag{83}$$

where

$$c''' = A(1) - c_{\rm nst} \tag{84}$$

with

$$c_{\rm nst} = c \int_0^1 dy\, y^{-1-\theta+\lambda} > 0. \tag{85}$$

To obtain the last equation, we used the dynamical susceptibility χ_D defined in Eq. (60) and the scaling form $\tilde{C}(x) \sim x^{-\lambda}$ given in Eq. (75) and assumed that t is large enough so that $L(t)/L_0 \ll 1$ holds. Note that $c_{\rm nst}$ represents the strength of the aging part of the response whose contribution to $\chi_{\rm ZFC}(t,0)$ scales as $c_{\rm nst} m^2/[L(t)/L_0]^\theta$. Now comparing the result (83) with (10) which reads as

$$\chi_{\rm FC} \equiv \lim_{t \to \infty} \chi_{\rm ZFC}(t,0)$$

we find the dynamical susceptibility χ_D defined in Eq. (60) is nothing but the desired FC susceptibility $\chi_{\rm FC}$. Thus using the inequality (62) we obtain

$$\chi_{\rm FC} = \chi_D > \chi_{\rm EA} \tag{86}$$

which is nothing but the anticipated inequality (16).

Lastly let us evaluate the TRM susceptibility in the aging regime. Suppose the waiting time t_w belongs to the mth epoch and observation is done well after the waiting time such that the domain growth proceeds appreciably $L(t) > L(t_w)$. Then summing over the aging part of the response (81) we obtain

$$\chi_{\rm TRM}(t = \tau + t_w, t_w) = \int_0^{t_w} dt' R(t,t')$$

$$\sim \sum_{k=1}^{m} \delta M_k(t)$$

$$\sim c'' \int_{L_0}^{L(t_w)} \frac{dL}{L} \frac{\tilde{\rho}(0) m^2}{\Upsilon (L/L_0)^\theta} \tilde{C}\left(\frac{L(t)}{L} \right)$$

$$\sim c_{\rm nst} \frac{m^2}{\Upsilon [L(t_w)/L_0]^\theta} \left(\frac{L(t)}{L(t_w)} \right)^{-\lambda}$$

$$\text{for} \quad L(t) \sim L(\tau) > L(t_w). \tag{87}$$

Here $c_{\rm nst}$ is defined above in Eq. (85) which represents the strength of the integral of the aging part of the response. To obtain the last equation, we used the scaling form $\tilde{C}(x) \sim x^{-\lambda}$ given in Eq. (75) and assumed that t_w is large enough so that $L_0/L(t_w) \ll 1$ holds. The functional form agrees with what was anticipated by Fisher and Huse.[15]

Thanks to the sum rule (9), the relaxation of TRM susceptibility (6) and ZFC susceptibility (7) can be obtained from each other using $\chi_{\rm ZFC}(t,0)$ obtained as Eq. (83). Here one must pay attention to the fact that $\chi_{\rm ZFC}(t,0)$ contains *both* the response due to droplets (which satisfy the FDT) and aging part (which violates the FDT) as can be seen in Eq. (83).

In the previous Secs. IV E 2 and IV E 3, we obtained scaling properties of the ZFC susceptibility in the quasiequilibrium/crossover regime. The ZFC susceptibility

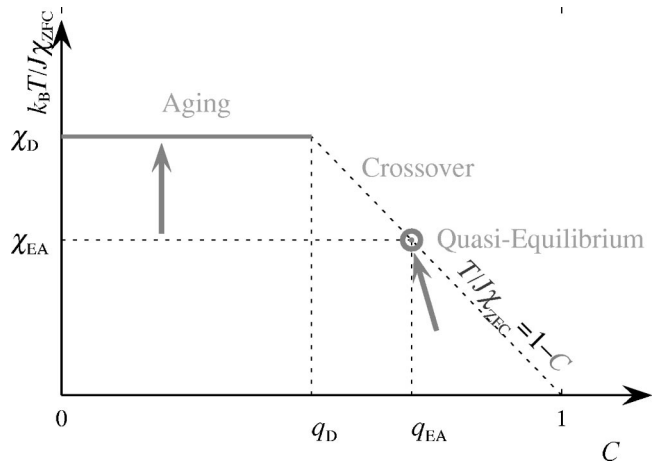

FIG. 3. Different asymptotic regimes in the $C-T\chi_{\mathrm{ZFC}}$ plane. The dotted line labeled $k_BT\chi=1-C$ represents the FDT line. See text for details.

in these regimes contain only response of droplets which satisfy the FDT. However, one can check that the TRM susceptibility in these regimes, which can be readily obtained via the sum rule, becomes a mixture of response due to droplets and aging part. Thus the ZFC susceptibility in the quasiequilibrium/crossover regimes is better suited to examine responses of droplets than the TRM susceptibility.

Conversely the TRM susceptibility in the aging regime is better suited to examine aging part of the response than the ZFC susceptibility. As can be seen in Eq. (87), the TRM susceptibility in the aging regime contains only the aging part of the response. On the other hand, one can check that the ZFC susceptibility which can be readily obtained by the sum rule becomes a mixture of response due to droplets and aging part.

6. Summary

Let us consider large time limit such that $L(t_w)\to\infty$ is taken with the ratio

$$x=\frac{L(\tau)}{L(t_w)} \tag{88}$$

being fixed to certain values. Here it is useful to consider the large time limit of the sum rule (9). For any τ that may be allowed to grow with t_w we find

$$\lim_{t_w\to\infty}[\chi_{\mathrm{TRM}}(\tau+t_w,t_w)+\chi_{\mathrm{ZFC}}\chi(\tau+t_w,t_w)]=\chi_D. \tag{89}$$

In the last equation we used the definition of the field cooled (FC) susceptibility defined in Eq. (10) and our result (86). The asymptotic behaviors discussed below are displayed in Figs. 2 and 3.

First $x<1$ corresponds to the quasi equilibrium regime, where the spin autocorrelation function slowly decays from 1 to static order parameter q_{EA} accompanying some weak waiting time dependence or weak violation of time translational invariance (TTI). Here if one fix $L(\tau)$ and let $L(t_w)\to\infty$ one obtains the ideal equilibrium limit behavior where the weak violation of TTI is removed. On the other hand, the FDT (18) $1-C(\tau+t_w,t_w)=k_BT\chi_{\mathrm{ZFC}}(\tau+t_w,t_w)$ is satisfied even in the presence of the weak violation of TTI. In the large time limit $L(t_w)\to\infty$ with fixed $x<1$, the time dependences (including the weak violation of TTI) disappears such that the spin autocorrelation converges to the static EA order parameter q_{EA} and the ZFC susceptibility converges to the equilibrium susceptibility $k_BT\chi_{\mathrm{EA}}$. Correspondingly the TRM susceptibility converges to $k_BT\chi_D-k_BT\chi_{\mathrm{EA}}=q_D-q_{\mathrm{EA}}$ because of the sum rule (89). In the last equation we used $k_BT\chi_D=1-q_D$ given in Eq. (60). To summarize, the spin autocorrelation function and the susceptibilities asymptotically become flat lines in the quasiequilibrium regime ($x<1$) as displayed in Fig. 2. In the parametric plot of Fig. 3, the whole quasi-equilibrium regime converges to a single point $(q_{\mathrm{EA}},k_BT\chi_{\mathrm{EA}})$. Importantly, the scaling theory has provided not only such asymptotic limits but details of finite-time (τ,t_w) correction terms by which the asymptotic limit is approached as discussed in Sec. IV E 2. The latter are well amenable to be examined seriously by experiments and simulations. In Sec. VII we present such a detailed analysis for the 4D EA model based on MC simulations.

Second $x\sim1$ corresponds to the crossover regime. From Eq. (69), we expect the spin autocorrelation function drops vertically [against $L(\tau)/L(t_w)$] from the EA order parameter q_{EA} down to the dynamical order parameter q_D which is smaller than q_{EA} due to the anomalously soft droplets. In this regime we expect the FDT (18) is still satisfied in spite of the strong nonstationary character and we expect the ZFC susceptibility increases vertically from the static susceptibility $k_BT\chi_{\mathrm{EA}}$ to a larger value $k_BT\chi_D=1-q_D$. Correspondingly the TRM susceptibility drops off vertically from $k_BT\chi_D-k_BT\chi_{\mathrm{EA}}=q_{\mathrm{EA}}-q_D$ to zero because of the sum rule (89). In the parametric plot of Fig. 3, the crossover regime converges to the line of points in the section of the FDT line between $(q_{\mathrm{EA}},k_BT\chi_{\mathrm{EA}})$ and $(q_D,k_BT\chi_D)$.

The abruptness of the changes of the two time quantities at $x\sim1$ is very surprising. Here let us recall the well known experimental[43] and numerical[44] observations that the so-called relaxation rate

$$S(\tau,t_w)\equiv\frac{d\chi_{\mathrm{ZFC}}(\tau+t_w,t_w)}{d\ln(\tau)} \tag{90}$$

has a broad peak centered at around $\tau\sim t_w$. Our scenario naturally suggests a modified relaxation rate function

$$S_{\mathrm{mod}}(x,t_w)\equiv\frac{d\chi_{\mathrm{ZFC}}(\tau+t_w,t_w)}{dx}\Big|_{x=L(\tau)/L(t_w)}, \tag{91}$$

which should have a sharper peak at $x\sim1$ with increasing $L(t_w)$. This modified relaxation rate will be useful for further numerical simulations and experiments.

In order to describe the interior of the crossover regime more closely, different scaling variables other than $L(\tau)$ and $L(t_w)$ are certainly needed. Unfortunately, the droplet theory which is based on the dynamical length scales cannot provide information for proper scaling variable to describe the interior of the crossover regime. A possible scaling variable

would be $\alpha=\tau/t_w$ as proposed by Fisher and Huse[15] with which the abruptness will be absent. Note that possible large time limits $t_w\to\infty$ classified by different values of α are smashed to a point $x=L(\tau)/L(t_w)=1$ in the x axis for all α.

Finally $x>1$ corresponds to the aging regime where the spin autocorrelation function takes a continuous value between q_D and 0 as deceasing function of x as given in Eq. (77). Here the result (87) implies the TRM susceptibility is asymptotically zero. The latter means the ZFC susceptibility converges to the FC susceptibility $k_BT\chi_{\rm FC}$ because of the sum rule (89). The FDT (18) is thus strongly violated. In the parametric plot of Fig. 3, asymptotic limit for each x converges to a point on the flat horizontal line connecting $(0,T\chi_D)$ and $(q_D,k_BT\chi_D)$.

In conventional understanding[7] which includes usual coarsening systems[35,36,41] and mean-field spin-glass models,[8] both the violation of TTI and FDT happens asymptotically at the same static order parameter $q_{\rm EA}$. A remarkable feature of our present scenario is that the break points of TTI and FDT are separated: the break point of TTI is located at $q_{\rm EA}$ while that of FDT is located at the dynamic order parameter q_D.

So far it is implicitly assumed that FDT (18) is valid in the quasiequilibrium regime and also in the crossover regime in spite of the fact that there are weak and strong waiting time effect. A supplementary argument for the validity of FDT can be made by considering the bound on the possible violation of FDT found in Ref. 32. The rigorous bound[32] on the integral violation $I(t,t_w)$ defined in Eq. (23) is put in terms of the entropy production rate which presumably has the same scaling form as the energy relaxation rate. Then using the scaling form of the energy relaxation (37) one finds

$$|I(t,t_w)|\leqslant K\int_{t_w}^{t}ds\,\sqrt{\frac{de(s)}{ds}}\leqslant K'[(t/t_0)^{1/2+\alpha}-(t_w/t_0)^{1/2+\alpha}] \tag{92}$$

with K and K' being certain finite constants and $0<\alpha\ll 1$ being an arbitrary small positive nonzero number. Now let us consider the bound in the large time limit $t_w\to\infty$ in the quasiequilibrium regime $x=L(\tau)/L(t_w)<1$. For convenience let us introduce y such that

$$\tau=t-t_w=t_0(t_w/t_0)^y. \tag{93}$$

Then we find

$$\lim_{t_w\to\infty} I(t,t_w)\leqslant(1/2+\alpha)K'\lim_{t_w\to\infty}(t_w/t_0)^{-1/2+y+\alpha}=0. \tag{94}$$

The last equations holds for $0\leqslant y<1/2$ since α is an arbitrary small positive number. This observation implies that FDT is satisfied not only in the equilibrium limit but also in the quasiequilibrium regime. In order to verify the validity of FDT in the crossover regime $y\sim 1$, apparently improved bounds are needed.

7. Comparison with conventional pictures

Finally, let us compare our scenario with the conventional picture for isothermal aging[7] which applies for the dynamical mean-field theory (MFT) of spin glasses[8] and usual coarsening systems.[35,36,41] Here let us consider the asymptotic limit $t_w\to\infty$ of the two time quantities by fixing the value of the autocorrelation function to a certain value C in the range $0<C<1$. In that limit, the ZFC susceptibility becomes a function of C, $\chi=\chi(C)$. This definition of asymptotic limit can be considered in general and our scenario implies the simple structure of $\chi(C)$ shown in Fig. 3. In the usual coarsening systems and in the dynamical MFT, the FDT line terminates at $(q_{\rm EA},T\chi_{\rm EA})$ while it extends up to $(q_D,T\chi_D)$ in our scenario. In the usual coarsening systems, a horizontal line connects $(0,k_BT\chi_{\rm EA})$ and $(q_{\rm EA},k_BT\chi_{\rm EA})$ where the FDT is violated strongly. On the other hand, the dynamical MFT predicts a curved line between $(0,\chi_D)$ and $(q_{\rm EA},\chi_{\rm EA})$. Our picture is different from both of them.

The difference between usual coarsening systems and our scenario is the presence of the anomalously soft droplets. Droplet excitations exist also in simple coarsening systems such as ferromagnets[34] but with extremely small probability. In our scenario, the anomalously soft droplet can exist with probability of order $O(1)$ in a given domain irrespective of the size of the domain so that the thermal fluctuations in each domain are anomalously large compared with equilibrium where there are no extended defects.

For clarity, let us note[42] that there are also some excessive response in usual coarsening systems due to thermalized domain walls[41] at wave numbers k such that $kL(t)\gg 1$. They are similar to the anomalously soft droplets in our scenario in the sense that (1) they satisfy FDT but (2) disappear in the ideal equilibrium. However their integral contribution to the response decreases with the growth of the domain $L(t)$ so that their contribution vanishes asymptotically. On the other hand, the excessive response of the anomalously soft droplets in our scenario give $O(1)$ contribution irrespective of the size of the domain so that their contribution to the response do not disappear as far as $t_w\to\infty$ limit (ideal equilibrium) is not took first.

Although both the dynamical MFT and our scenario concludes the inequality (16) $\chi_{\rm FC}>\chi_{\rm EA}$, the origins are different. The difference between the two, called *anomaly*, is attributed to contributions of aging part of the response function which violates the FDT in the case of the dynamical MFT while it is rather attributed to the responses due to the anomalously soft droplets which still satisfy the FDT in our scenario. For example, one can see in Eq. (83) that $\chi_{\rm FC}$ $(=\chi_D)$ is generated not from the aging part but from the part due to the anomalously soft droplets which satisfies the FDT.

There is a conjecture[33] that there is a connection between the statics and dynamics such that the function $\chi=\chi(C)$ in the dynamics should be related to the overlap distribution function $P(q)$ in equilibrium, as

$$k_BT\chi(C)=\int_C^1 dC'\int_0^{C'}dC''P(C''). \tag{95}$$

This is known to hold exactly in some (not all) mean-field models[8] and usual coarsening systems.[36,41] Moreover, an interesting conjecture[45] was proposed recently that at finite time (length) scales, the above formula holds for the two

time quantities at a finite waiting time t_w and a $P(q)$ measured in equilibrium of a finite system of size $L(t_w)$. We agree with this proposal partially but not completely as we discuss in the following.

In order to fully reproduce the parametric plot Fig. 3, we would need $P(q)$ with a delta peak at $q=q_D$ rather than at $q=q_{\rm EA}$. On the other hand, we expect a $P(q)$ with delta peak at $q=q_{\rm EA}$ in the absence of any extended defects as the original droplet theory has predicted.[14] Thus the correspondence between the dynamics and statics does not hold at all in this sense in our scenario.

However, one can explicitly consider a rather special static situation in the presence of extended defects of size, say *R*, which is actually what we considered in Sec. IV D. In any finite size systems, it is likely that the existence of boundaries (periodic, free, etc.) will intrinsically induce certain defects as compared with infinite systems.[22,46,47] Thus we expect actually the circumstance we are considering is relevant in practice. Our scenario implies the average overlap $\overline{q}=\int_0^1 dqqP(q)$ measured in such an equilibrium is equivalent to $q(R,R)=q_D+\tilde{\rho}(0)m^2k_BT/\Upsilon(R/L_0)^{\theta}A(1)$ of Eq. (58). Thus our scenario suggests $\chi_{\rm FC}=\lim_{\tau\to\infty}\chi_{\rm ZFC}(\tau+t_w,t_w)=1-\overline{q}=1-\int_0^1 dqqP(q)$ for any t_w while $\lim_{\tau\to\infty}C(\tau+t_w,t_w)\to 0$ for any t_w. Thus our scenario agrees with the conjecture of Ref. 45 at the special point $C=0$ plus the usual FDT part between $C=q_{\rm EA}$ and $C=1$ but not in the section $0<C<q_{\rm EA}$. Here $P(q)$ should be understood as measured in equilibrium but with the extended defects. It will be natural to expect that $P(q)$ in such a situation becomes a nontrivial, non-self-averaging function of q with finite amplitude at $q=0$ as observed in many numerical simulations of finite size systems.[48,49]

In the above arguments, we considered asymptotic limits with fixed *C* while it is more natural to consider asymptotic limits with fixed ratio of the two length $x=L(\tau)/L(t_w)$ in the droplet theory. In the dynamical MFT, one needs infinitely many kinds of time reparametrization functions $h(t)$ to span the whole correlation range $0<C<1$ but the droplet theory has only one natural variable $L(t)$. However, it should be remarked that the scaling variable to describe the interior of the crossover regime $q_D<C<q_{\rm EA}$ is not known at present within the droplet theory.

V. GROWTH LAW OF THE CORRELATION LENGTH IN OFF-EQUILIBRIUM

As discussed in Sec. IV, the dynamical length scale $L(t)$ and its growth law with time are important to understand nature of aging in SG systems from the view point of the scaling theory. In the present section, we discuss our numerical results of the length scale and its growth law during isothermal aging. A plausible definition of the length scale $L(t)$ is given by a decay constant of a correlation function $G(r,t)$. We measure the equal-time replica correlation function in off-equilibrium under zero magnetic field, defined by

$$G(r,t)=\sum_i \langle S_i^{(\alpha)}(t)S_i^{(\beta)}(t)S_{i+r}^{(\alpha)}(t)S_{i+r}^{(\beta)}(t)\rangle, \qquad (96)$$

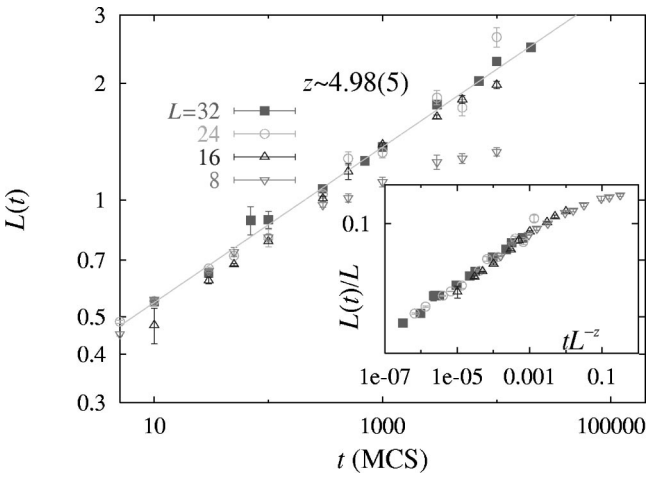

FIG. 4. $R(t)$ of the 4D Ising SG model at $T/J=2.0$ with different system sizes. The dashed line represents a power law with exponent $1/z$. In the inset, an expected finite-size scaling plot is shown.

where α and β denote the replica indices which are updated independently from different initial random spin configurations. In our simulation, only one MC sequence is performed for each random bond. Typical number of samples averaged over bond realizations is about 128. As reported previously,[20,22,50] the correlation function $G(r,t)$ exhibits a complicated functional form which is not a simple exponential and depends on time *t*. This may be because a characteristic distance above which $G(r,t)$ approximately follows an exponential form depends on time considerably. In order to avoid the artificial effect, we do not employ the so-called ratio method,[22,50] where the full data of $G(r,t)$ are used independent of *t*. Instead, we estimate $L(t)$ by fitting directly the tail part of $G(r,t)$ to an exponential formula for each time *t*. In the fitting procedure, we focus our attention only on the large distance tail of $G(r,t)$ and carefully choose the range depending on time *t*.

In Fig. 4 we show our results of the length scale $L(t)$ at the critical temperature $T_c=2.0J$. The data of the length scale $L(t)$ follows expected critical power law (30) except for the data with $L=8$, which is due to finite-size effect. The estimate of the exponent *z*, 4.98(5), is roughly consistent with that of the previous work,[27] which quoted $z=4.45(1)$. The data, including the size $L=8$ deviated from the power law, scale well using a standard finite-size scaling form, shown in the inset of Fig. 4. It is seen that the length scale $L(t)$ manages to reach at most few lattice spacing even at about 10^5 MCS. Nonetheless it should be noted that $L(t)$ already captures macroscopic behavior in the sense that the critical exponent *z* is successfully estimated from $L(t)$ and that a strong finite-size effect is observed already in $L=8$ data.

Let us now examine the crossover from critical to activated dynamics discussed in Sec. IV B. In Fig. 5, we display the raw data of the length scale $L(t)$ below T_c and at T_c. The critical dynamics is expected to be dominant near T_c. In fact, the length scale $L(t)$ at $T/J=1.8$ is not distinguishable from that at $T=T_c$ within our time regime. Let us examine the

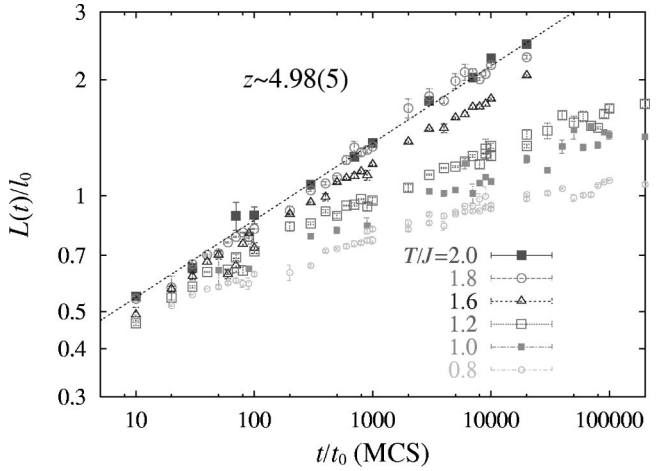

FIG. 5. Time evolution of $R(t)$ of the 4D Ising SG model at T_c and below T_c with $L=24$.

crossover scaling defined in Eqs. (34) and (35). We present the scaling plot in Fig. 6 by using the same data as shown in Fig. 5. In this plot, for two scaling parameters, T_c and ν, we use the known values obtained previously,[25] while only one remaining parameter ψ is appropriately chosen for the data with different temperatures to merge into a universal curve. The best scaling plot is obtained by $\psi \sim 2.5-3.0$. The proposed scaling pretty well works in the observed time regime. It is clearly found that the scaling function exhibits a crossover from the critical power law to slower growth law associated with low temperature dynamics which is compatible with the logarithmic growth law predicted by the droplet theory.

VI. RELAXATION OF ENERGY AND DENSITY OF DOMAIN WALL

In the present section, we examine scaling properties of one-time quantities under isothermal aging after quench

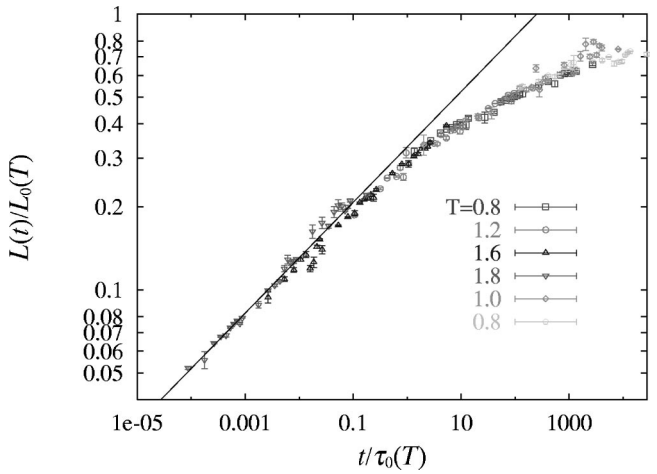

FIG. 6. Scaling plot of $R(t)$ of the 4D Ising SG model, where the SG transition temperature $T_c=2.0$ and the critical exponent $\nu=0.93$ are fixed, but the dynamical exponent z is obtained to be 4.98(5) from the best scaling.

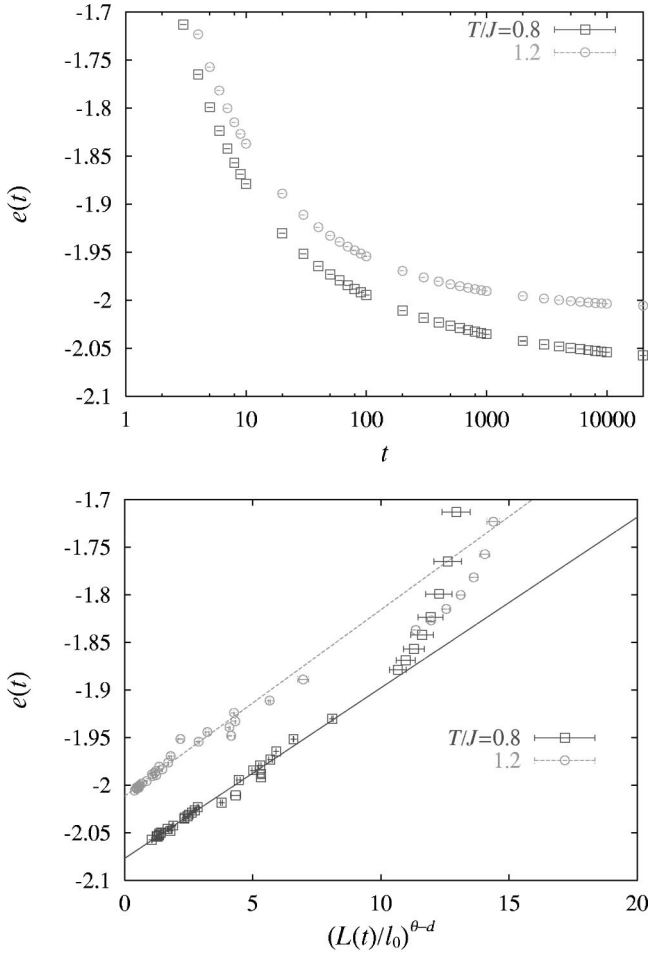

FIG. 7. Energy relaxation at $T/J=0.8$ and 1.2 as a function of elapse time (upper figure) and the length scale $L(t)$ (lower figure). The straight lines in the lower figure represent fitting result to a linear function function of $[L(t)/l_0]^{\theta-d}$.

based on the view point presented in Sec. IV C. In the following sections, we perform simulations mainly at two low temperatures $T/J=1.2$ and 0.8 which amount to $0.6T_c$ and $0.4T_c$, respectively. It is found that the effects of critical fluctuations do not dominate our time window at these temperatures but can be taken into account in a renormalized way.

A. Energy

In Fig. 7, we present the data of the energy per spin $e(t)$ defined in Eq. (36) at $T/J=0.8$ and 1.2. As seen in the upper figure, the energy function relaxes with time to an equilibrium value at each temperature. However, it is rather hard to extract the equilibrium value from the figure because of the extremely slow dynamics. On the other hand, the scaling formula (37) says that the energy approaches its equilibrium value linearly as a function of $L^{\theta-d}(t)$. We thus plot the same data set against $L^{\theta-d}(t)$ in the lower one by using the length scale $L(t)$ estimated independently in the previous section and the known value of the stiffness exponent $\theta=0.82$.[25] We see the linear behavior as a function of $L^{\theta-d}(t)$

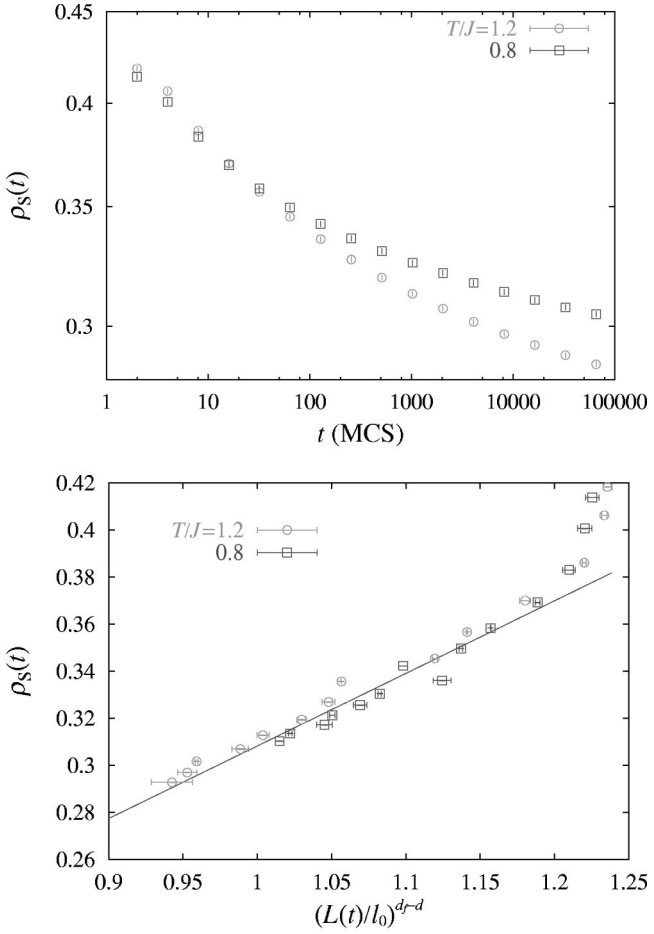

FIG. 8. Density of the domain wall at $T/J=0.8$ and 1.2 with $L=24$ as a function of time t (upper figure) and $L(t)$ (lower figure). The straight line in the lower figure represents fitting result to a linear function of $L^{d_f-d}(t)$ with $d_f=3.75$ (Ref. 51).

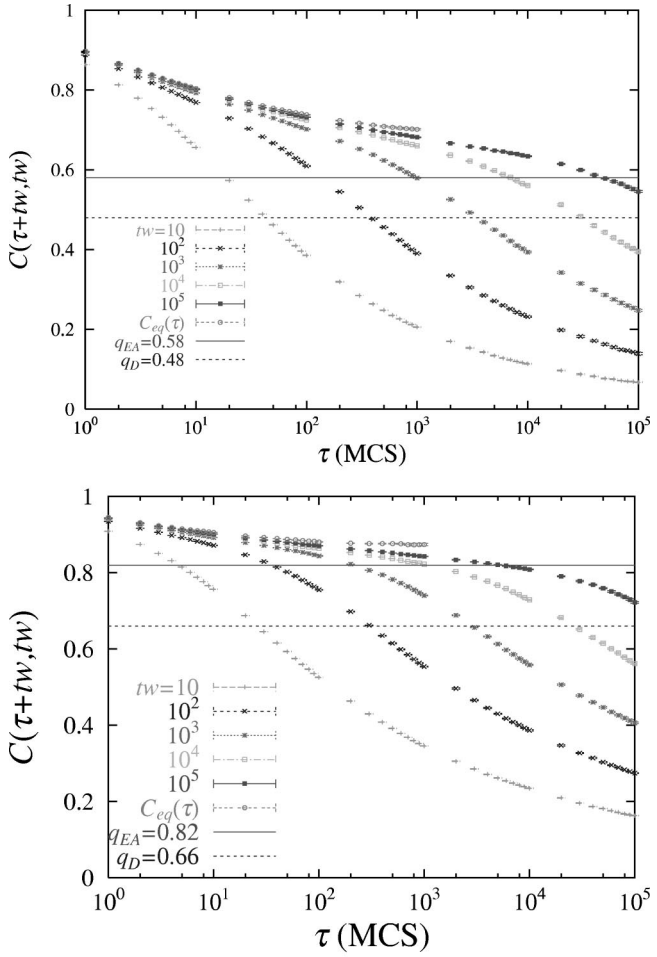

FIG. 9. Spin autocorrelation function of the 4D Ising SG model at $T/J=1.2$ (upper figure) and 0.8 (lower figure) with different waiting time. The top data curves are the equilibrium curves obtained in Sec. VII C.

for large $L(t)$ which supports the validity of the scaling formula (37). One can take the long time limit of the energy relaxation using the scaling formula. A similar scaling analysis of the energy has been confirmed in the 3D Ising EA SG model including finite size effects.[22] This two stroke strategy has an advantage over the direct analysis with time and gives us a more powerful tool in the analysis of two-time quantities discussed in the following sections.

B. Density of domain wall

In Fig. 8, we show the domain-wall density $\rho_s(t)$ defined in Eq. (39). The average over bond realizations is taken over 256 samples with $L=24$. It is found that the density monotonically decays and there is no tendency of saturation, which is similar behavior observed in the 3D Ising EA model.[21] This is clearly seen in the lower figure, where following Eq. (38) we plot $\rho_s(t)$ as a function of $L^{d_f-d}(t)$ estimated in the previous section. Here we use the value of the fractal dimension $d_f=3.75$ recently evaluated in Ref. 51. As shown in the lower figure, $\rho_s(t)$ is well fitted by a linear function of $L^{d_f-d}(t)$ and the fitting function is down to zero in the large time/length limit. We stress again the validity of the scaling formula with the length scale $L(t)$.

VII. RELAXATION OF CORRELATION FUNCTION AND LINEAR SUSCEPTIBILITIES

We now turn to the two time quantities. First we display the data in Sec. VII A and discuss the overall features qualitatively in Sec. VII B from the point of view of the scaling theory explained in Sec. IV E. Then we go to more detailed examinations of the scaling properties in the subsequent sections. In order to test the scaling ansatz explained in Sec. IV E which are expressed in terms of the dynamical length scale $L(t)$, we use the data of $L(t)$ discussed in the previous Sec. V.

A. Measurements of spin autocorrelation function and linear susceptibilities

In Fig. 9, we present the data of the spin autocorrelation function $C(\tau+t_w,t_w)$ measured up to 10^5 MCS for various waiting times $t_w=10,10^2,10^3,10^4,10^5$ at $T/J=1.2$ and 0.8. The system size is $L=24$. The data are obtained by performing MC simulations starting from random initial conditions. The average over realizations of randomness is taken over 32 samples. The data show clear waiting time dependences. We

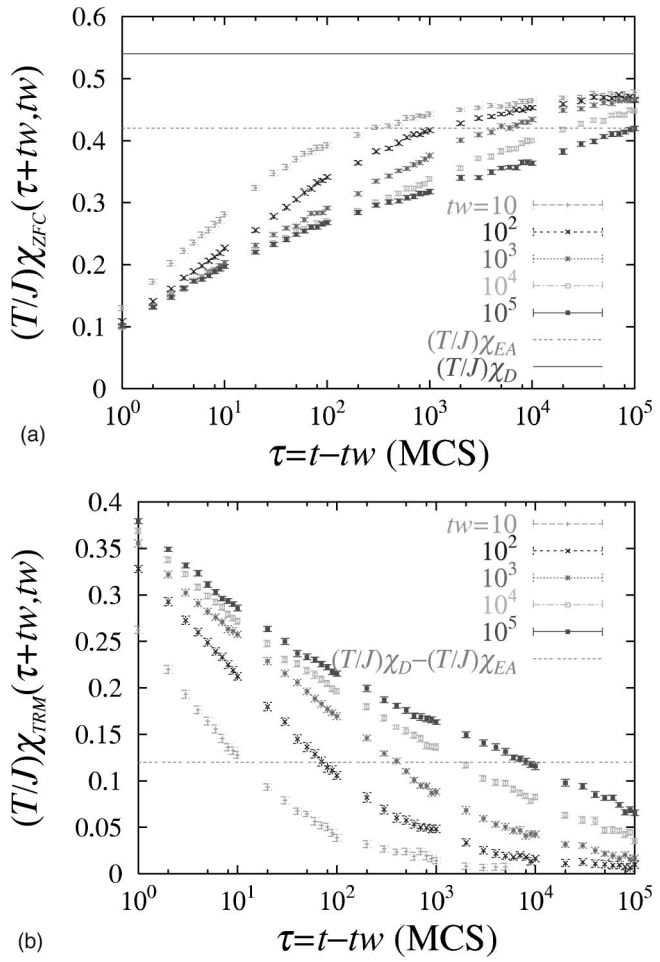

FIG. 10. Linear susceptibilities at $T/J=1.2$: ZFC susceptibility (upper figure) and TRM susceptibility (lower figure). Here $(T/J)\chi_{\mathrm{EA}}=0.42$ and $(T/J)\chi_D=0.52$.

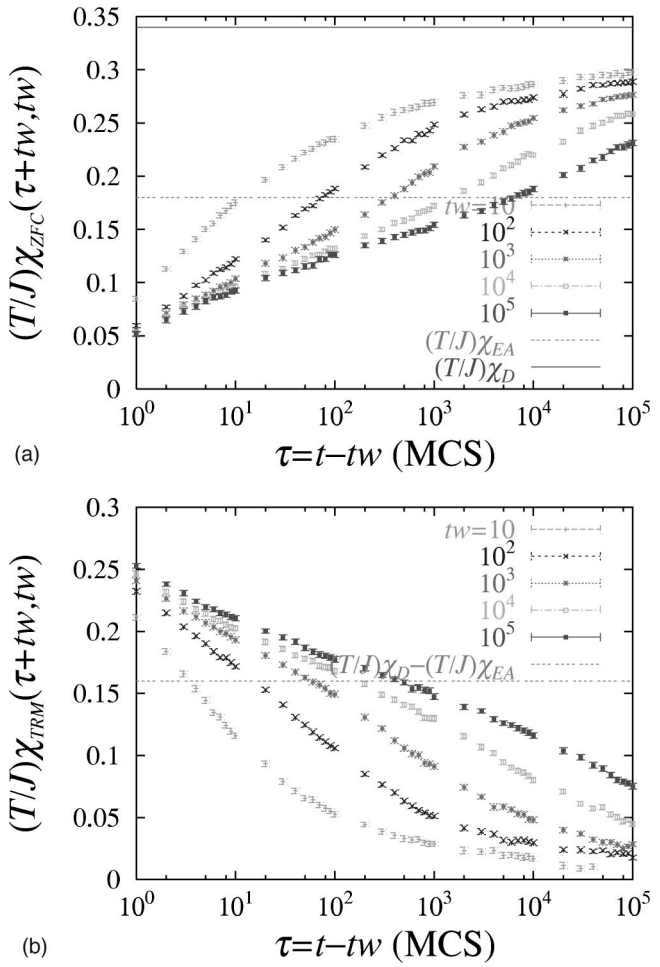

FIG. 11. Linear susceptibilities at $T/J=0.8$. Here $(T/J)\chi_{\mathrm{EA}}=0.2$ and $(T/J)\chi_D=0.33$.

also show the curve of equilibrium relaxation $C_{\mathrm{eq}}(\tau)$ extracted in the analysis which will be explained later in Sec. VII C. The latter yields the value of static EA order parameter q_{EA} whose value is also indicated in the figure. In addition we also indicate in the figures the values of the dynamical order parameter q_D which will be obtained in the analysis explained later in Sec. VII E. As discussed in Sec. IV E, we expect that the spin autocorrelation function develops a plateau at q_{EA} in the quasiequilibrium regime and decays down to zero in the aging regime. The decay is expected to be most steep at around the dynamical order parameter q_D. The data indeed appears qualitatively compatible with these expectations.

In Figs. 10 and 11, we display the data of the ZFC susceptibility $(T/J)\chi_{\mathrm{ZFC}}(\tau+t_w,t_w)$ and the TRM susceptibility $(T/J)\chi_{\mathrm{TRM}}(\tau+t_w,t_w)$ measured up to 10^5 MCS for various waiting times $t_w=10,10^2,10^3,10^4,10^5$ at $T/J=1.2$ and $T/J=0.8$ using field of strength $h/J=0.1$. Again the system size is $L=24$. The average over realizations of randomness is taken over 32 samples. Here the susceptibilities are defined by dividing the measured magnetization per spin $m(t)=(1/N)\Sigma_{i=1}^{N}S_i(t)$ at time t by the strength of the external magnetic field h/J. For the measurement of the TRM susceptibility $\chi_{\mathrm{TRM}}(t=\tau+t_w,t_w)$, some waiting time t_w is elapsed under the field and then the field is switched off at $t=t_w$. Conversely, the ZFC susceptibility $\chi_{\mathrm{ZFC}}(t=\tau+t_w,t_w)$ is measured by first elapsing the waiting time t_w with no applied field and then field is switched on at $t=t_w$.

To check the linearity of the response, we examined the sum rule (9): the sum of the two susceptibilities become $(T/J)\chi_{\mathrm{ZFC}}(t,0)$. As shown in Fig. 12, the sum rule is satisfied over our time window within the statistical accuracy.

In Figs. 10 and 11, we can see clear waiting time dependences of the susceptibilities. As discussed in Sec. IV E, we expect that the ZFC susceptibility first develops a plateau at the static susceptibility χ_{EA} within the quasiequilibrium regime and then grows further up to the dynamical susceptibility χ_D later in the aging regime. Correspondingly, we expect that the TRM susceptibility develops a plateau at $\chi_D-\chi_{\mathrm{EA}}$ within the quasiequilibrium regime and decays down to zero in the aging regime. For the references, we indicated the values of the static susceptibility $(T/J)\chi_{\mathrm{EA}}$, the dynamical susceptibility $(T/J)\chi_D$, and their difference in the figures using the values which will be obtained in Secs. VII C and VII E. The data indeed appears qualitatively compatible with the expected behavior.

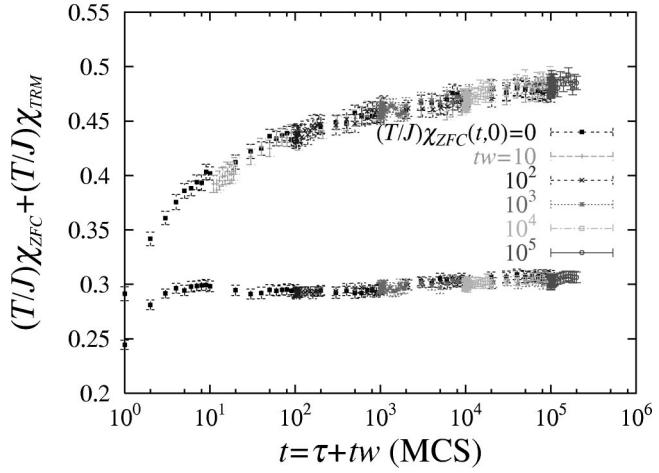

FIG. 12. Check of the sum rule (9) at $T/J=1.2$ (upper figure) and 0.8 (lower figure). The data of the ZFC susceptibility $(T/J)\chi_{\rm ZFC}(t,0)$ is also included.

B. Overall features

In Fig. 13, we show the spin autocorrelation function $C(\tau+t_w,t_w)$ and the ZFC susceptibility $1-(T/J)\chi(\tau+t_w,t_w)$ plotted against $x=L(\tau)/L(t_w)$.

Here we parametrized the times τ and t_w using the time-dependent length $L(t)$ obtained in Sec. V. More precisely, we first fitted the data of the domain size $L(t)$ as $L(t)/L_0=a_0+a_1\ln(t)+a_2\ln^2(t)+a_3\ln^2(t)$ with t measured in the unit of MCS and $L_0=1$ (lattice distance). This fitting was enough to model the data of $L(t)$ within our time window. Then we used the resultant fitting functions to do the paramterization here and in the following analysis. When we do the parametrization, we discard short time data $t<10$ because $L(t)$ is not available there.

The figure should be compared with Fig. 2 which explains the expected asymptotic behavior of the two time quantities in the large time limit $L(t_w)\to\infty$ with the ratio $x=L(\tau)/L(t_w)$ fixed to certain values. We expect three distinct regimes depending on the value of the fixed ratio (i) quasiequilibrium regime $x<1$ where the autocorrelation functions spans values in the range $q_{\rm EA}<C<1$, (ii) crossover regime $x\sim1$ for $q_D<C<q_{\rm EA}$, and (iii) aging regime $x>1$ for $0<C<q_D$. Here $q_{\rm EA}$ and q_D are convergence points of the break points of TTI and FDT, respectively, in the limit $L(t_w)\to\infty$.

In the quasiequilibrium regime $x<1$, we expect that the spin autocorrelation function convergence to a plateau $q_{\rm EA}$ in the large time limit $L(t_w)\to\infty$. Correspondingly the ZFC susceptibility $(T/J)\chi_{\rm ZFC}(\tau+t_w,t_w)$ is expected to converge to the static susceptibility $(T/J)\chi_{\rm EA}=1-q_{\rm EA}$. In the figure, we indicated the value of $q_{\rm EA}$ which will be obtained later in Sec. VII C. The data indeed appears descending down toward the plateau from above with increasing t_w (at $x<1$) but still far from it. Fortunately, the scaling theory provides prediction on the correction terms to the asymptotic limit as explained in Sec. IV E 2. In the Sec. VII C, we will examine the correction terms in detail which actually yields the value of $q_{\rm EA}$. Second important observation is that the FDT $1-C(t,t_w)=(T/J)\chi_{\rm ZFC}(t,t_w)$ is well satisfied in the quasiequilibrium regime $x<1$ as expected.

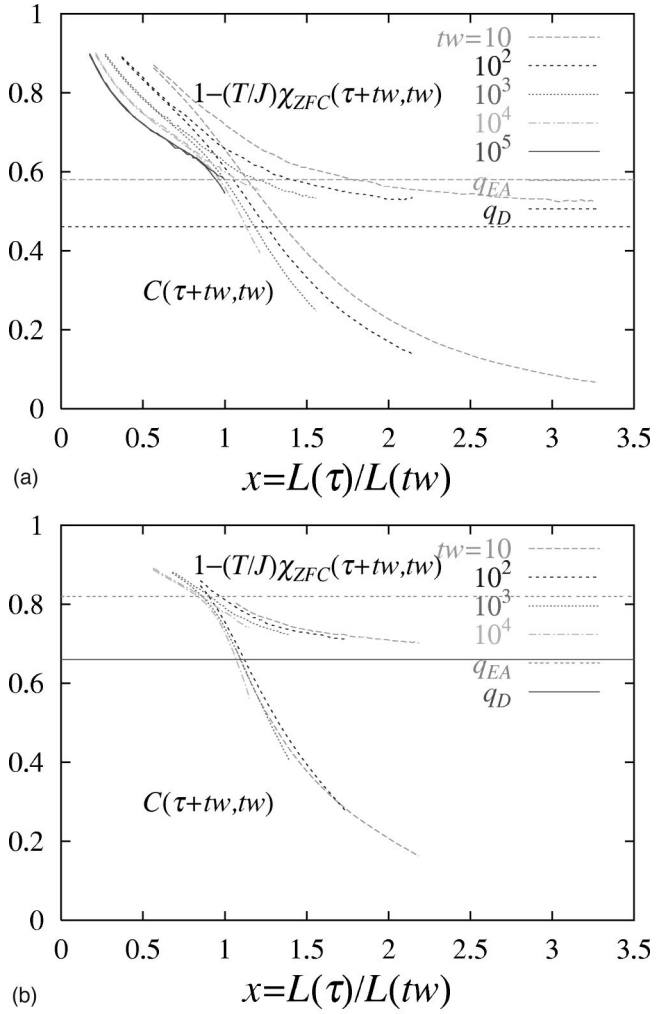

FIG. 13. Plot of spin autocorrelation function $C(\tau+t_w,t_w)$ and $1-(T/J)\chi_{\rm ZFC}(\tau+t_w,t_w)$ against $x=L(\tau)/L(t_w)$ at $T/J=1.2$ (upper figure) and 0.8 (lower figure). For each waiting time t_w, the lower curve is the spin autocorrelation function and the upper curve is the susceptibility.

In the crossover regime $x\sim1$, we expect a vertical drop from the plateau at the static EA order parameter $q_{\rm EA}$ down to the dynamical order parameter q_D for the spin autocorrelation function. Correspondingly the ZFC susceptibility $(T/J)\chi_{\rm ZFC}(\tau+t_w,t_w)$ is expected to jump from the static susceptibility $(T/J)\chi_{\rm EA}=1-q_{\rm EA}$ up to the dynamical susceptibility $(T/J)\chi_D=1-q_D$ still keeping the FDT $1-C(t,t_w)=(T/J)\chi_{\rm ZFC}(t,t_w)$ as explained in Sec. IV E 2. In the figure, we indicated the value of q_D which will be obtained later in Sec. VII E. We will examine the slope of the curves around $x\sim1$ in Sec. VII E and find indeed that the suitably refined relaxation rate function $S_{\rm mod}(x,t_w)$ defined in Eq. (91) have a sharply pronounced peak at around $x\sim1$. Furthermore, we will examine the violation of FDT $I(\tau+t_w,t_w)=1-C(\tau+t_w,t_w)-(T/J)\chi_{\rm ZFC}(\tau+t_w,t_w)$ defined in Eq. (23) in Sec. VII G and find indeed that it is decreasing with increasing t_w in the crossover regime x

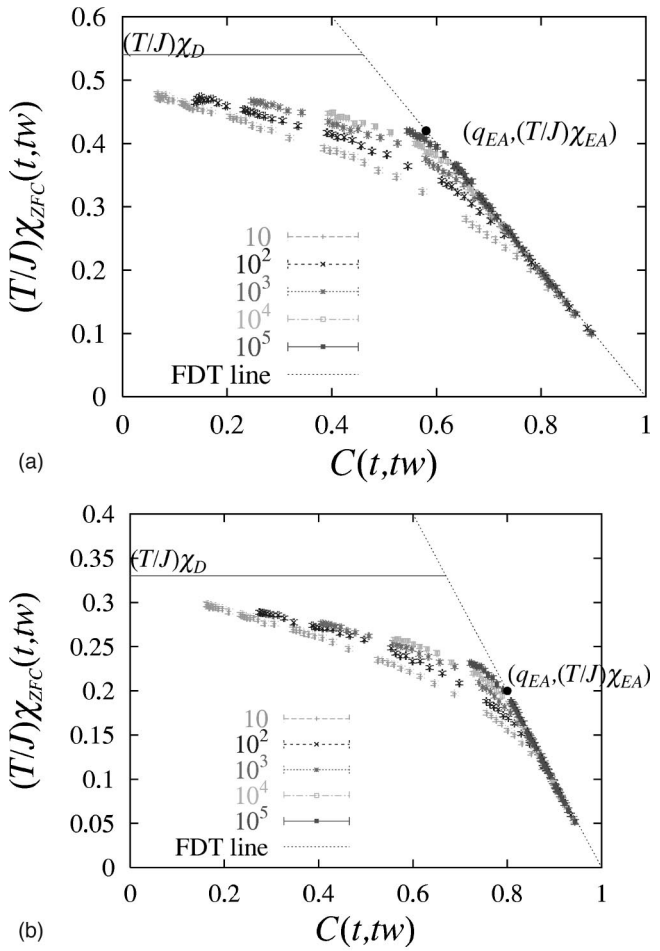

FIG. 14. Parametric plot $(T/J)\chi_{\mathrm{ZFC}}(t,t_w)$ vs $C(t,t_w)$ at $T/J=1.2$ (upper figure) and 0.8 (lower figure). The straight tangent lines represents the FDT (18). The convergence points of the break points of TTI $[q_{\mathrm{EA}},(T/J)\chi_{\mathrm{EA}}]$ and the break points of FDT $[q_D,(T/J)\chi_D]$ which will be obtained later in Secs. VII C and VII E, respectively, are indicated.

~ 1. The result is compatible with our expectation that the FDT is asymptotically valid even in the crossover regime.

In the aging regime $x>1$, we expect the ZFC susceptibility $1-(T/J)\chi_{\mathrm{ZFC}}(\tau+t_w,t_w)$ converges to the dynamical susceptibility $(T/J)\chi_D=1-q_D$ while spin autocorrelation function $C(\tau+t_w,t_w)$ becomes a scaling function of $L(\tau)/L(t_w)$. Indeed the data appears slow converges to such limits. For the susceptibility, the scaling theory provides prediction on the scaling forms of the correction terms to the asymptotic limit as explained in Sec. IV E 5. We will examine and confirm them in Sec. VII E. The value of q_D indicated in Fig. 13 will be actually obtained as the result of such an analysis.

In Fig. 14, the susceptibility $(T/J)\chi_{\mathrm{ZFC}}(\tau+t_w,t_w)$ and the spin autocorrelation function $C(\tau+t_w,t_w)$ are plotted in a parametric way. It should be compared with Fig. 3, which explains the expected asymptotic regimes in the large time limit $L(t_w)\to\infty$ with the fixed ratio $x=L(\tau)/L(t_w)$. The curves apparently continue to move upwards with increasing waiting time t_w and the break point of FDT does not appear

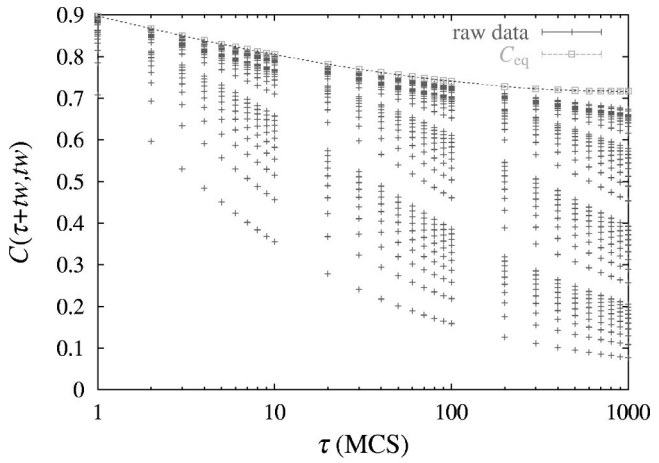

FIG. 15. Spin autocorrelation function at $T/J=1.2$. The top data points are the equilibrium limit obtained by the extrapolation method explained in the text.

to converge to $[q_{\mathrm{EA}},(T/J)\chi_{\mathrm{EA}}]$ which will be obtained in Sec. VII C. This observation is consistent with our picture presented in Fig. 3. It is radically different from conventional understanding[7] that assumes break points of TTI and FDT are the same. As we discuss in Sec. VII F, the separation of the break points of TTI and FDT will become apparent when time (length) dependences are explicitly considered.

C. Quasiequilibrium regime

Let us now examine the scaling properties in the quasiequilibrium regime $x=L(\tau)/L(t_w)<1$ discussed in Sec. IV E 2. Since we have seen the FDT is well satisfied in the quasiequilibrium regime $x<1$ (see Fig. 13), we will only use the data of the spin autocorrelation function. To focus on the quasiequilibrium regime, we took another dense data set of the autocorrelation function $C(\tau+t_w,t_w)$ (shown in Fig. 15) of many waiting times $t_w=1,\ldots,30\,000$ (MCS) and relatively short time separations $\tau<1000$ (MCS). Here we do not use the fitting of the growth law of $L(t)$ to parametrize the time but use directly the data of $L(t)$ obtained in Sec. V.

The formula (67) combined with Eq. (65) gives a protocol to extract the static EA order parameter as the following. This analysis is already reported partly in our previous work.[17]

At first we take the equilibrium limit $t_w\to\infty$ of $C(\tau+t_w,t_w)$ for each time separation τ. From Eq. (67), one finds that the autocorrelation function becomes only a linear function of $1/L^{d-\theta}(t_w)$ for a fixed τ. Thus we plotted the data points of a given τ of various t_w against $1/L^{d-\theta}(t_w)$ and fitted to a linear function in the large $L(t_w)$ regime. The equilibrium limit $C_{\mathrm{eq}}(\tau)$ is read off directly from the fit. Here we use the stiffness exponent $\theta=0.82$.[25] For $L(t_w)$ we used the data obtained in Sec. V. Typical fitting results are shown in Fig. 16. The linearity as a function of $1/L^{d-\theta}(t_w)$ supports the validity of the formula (67). We repeated the same procedure for each τ. The obtained equilibrium curve $C_{\mathrm{eq}}(\tau)$ was displayed in Fig. 9.

Next we take the large τ limit of the extracted $C_{\mathrm{eq}}(\tau)$ using Eq. (65). As shown in Fig. 17, $C_{\mathrm{eq}}(\tau)$ appears as a

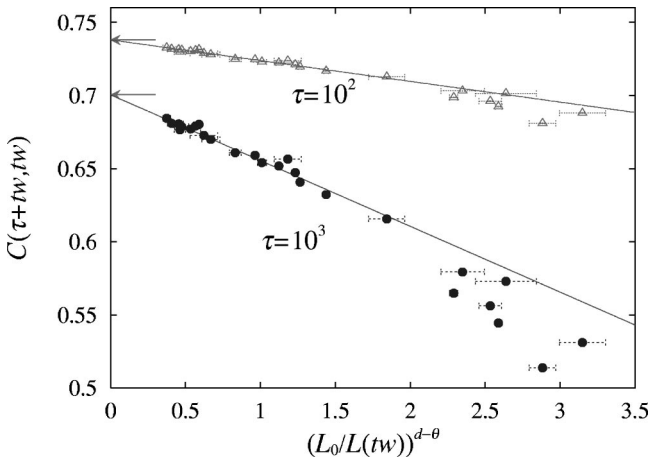

FIG. 16. Typical examples of the extrapolation to the long t_w limit with fixed τ. Two arrows represent the extrapolated values of $C_{\rm eq}(\tau)$ of $\tau=100$ and 1000 at $T/J=1.2$. The horizontal error bars are those of $L(t)$ presented in Fig. 5.

linear function of $1/L^{\theta}(\tau)$ which supports Eq. (65). A linear fit gives the EA order parameter $q_{\rm EA}$ as the limiting value. We obtained the EA order parameter $q_{\rm EA}=0.58(2)$ at $T/J=1.2$ and 0.82(1) at $T/J=0.8$. To our knowledge this and our previous work[17] is the first which confirmed this fundamental scaling law (65).

Finally, we discuss the weak nonequilibrium correction term to the equilibrium limit which is responsible for the weak violation of TTI in the quasiequilibrium regime. The expression (67) suggests that the weak nonequilibrium correction term $\Delta C(\tau+t_w,t_w)=C(\tau+t_w,t_w)-C_{\rm eq}(\tau)$ multiplied by $L^{\theta}(\tau)$ becomes only a function of $L(\tau)/L(t_w)$ (<1). As shown in Fig. 18, we confirm this scaling form. For the limit of $L(\tau)/L(t_w)\ll 1$, the scaling function shows the expected power law behavior $[L(\tau)/L(t_w)]^{d-\theta}$ being consistent with Eq. (67).

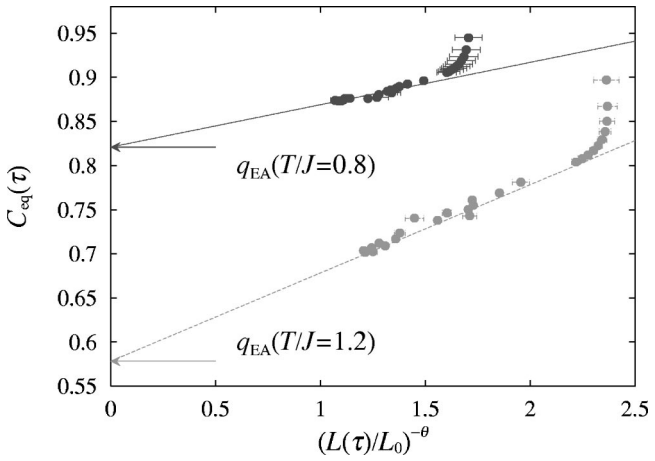

FIG. 17. Equilibrium spin autocorrelation function $C_{\rm eq}(\tau)$ at $T/J=1.2$ (upper data)and 0.8 (lower data). The horizontal error bars are those of $L(t)$ presented in Fig. 5. The lines represent fittings according to the formula (65).

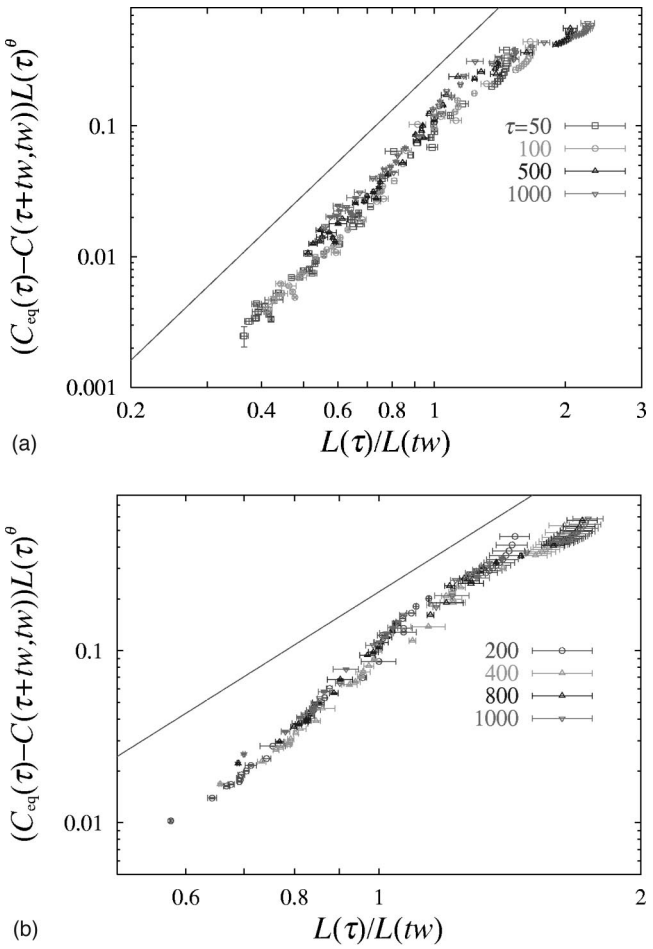

FIG. 18. Scaling plot of the non-equilibrium correction terms of $C(\tau+t_w,t_w)$ in the quasi-equilibrium regime at $T/J=1.2$ (upper figure) and 0.8 (lower figure). The horizontal error bars are those of $L(t)$ presented in Fig. 5. The line has the expected slope $d-\theta$ for small $L(\tau)/L(t_w)$ limit [see Eq. (67)].

D. Crossover regime

In the crossover regime $x=L(\tau)/L(t_w)\sim 1$, we expect a vertical jump of the two time quantities at asymptotic limit $L(t_w)\to\infty$. In Fig. 19 we display the plot of the usual relaxation rate function $S(\tau,t_w)$ of Eq. (90), which shows the well known peak structure observed in experiments[43] and a MC simulation.[44] This can be interpreted as the signal of the rapid changes in the crossover regime. However, our scenario naturally suggested a more appropriate, *modified* relaxation rate function $S_{\rm mod}(x,t_w)$ of Eq. (91). In Fig. 20 we show the plot of the modified relaxation rate function. It clearly develops a sharp peak at around $x\sim 1$ with increasing $L(t_w)$ as expected.

E. Scaling of susceptibilities

For the growth of the ZFC susceptibility with zero waiting time we expect a scaling form (83) which reads

$$\chi_{\rm ZFC}(t,0)\sim\chi_D-c'''m^2\frac{m^2}{\Upsilon(L(t)/L_0)^{\theta}}$$

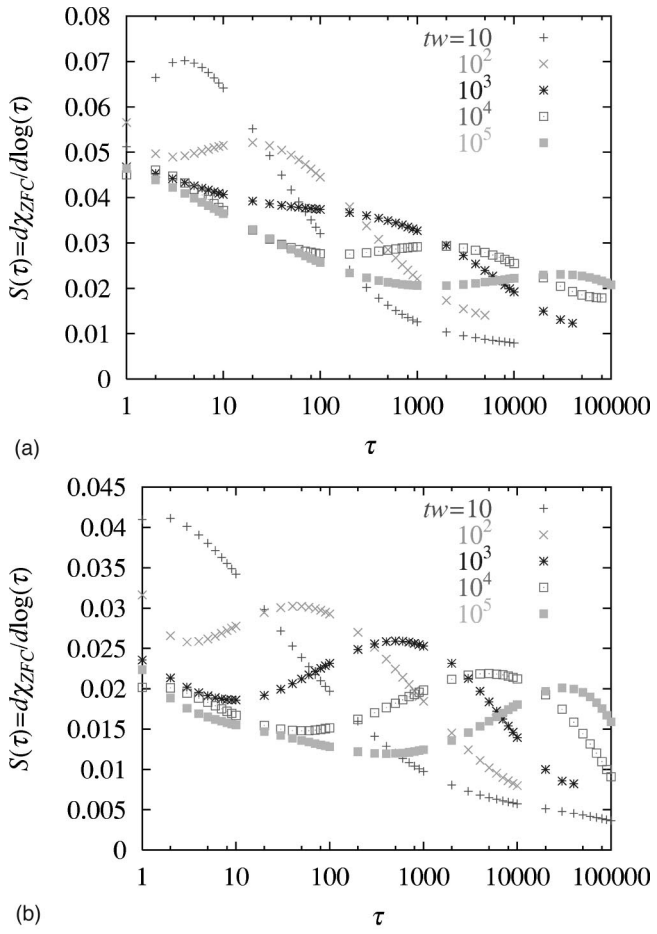

FIG. 19. Plot of the usual relaxation rate function $S(\tau,t_w)$ at $T/J=1.2$ (upper figure) and 0.8 (lower figure).

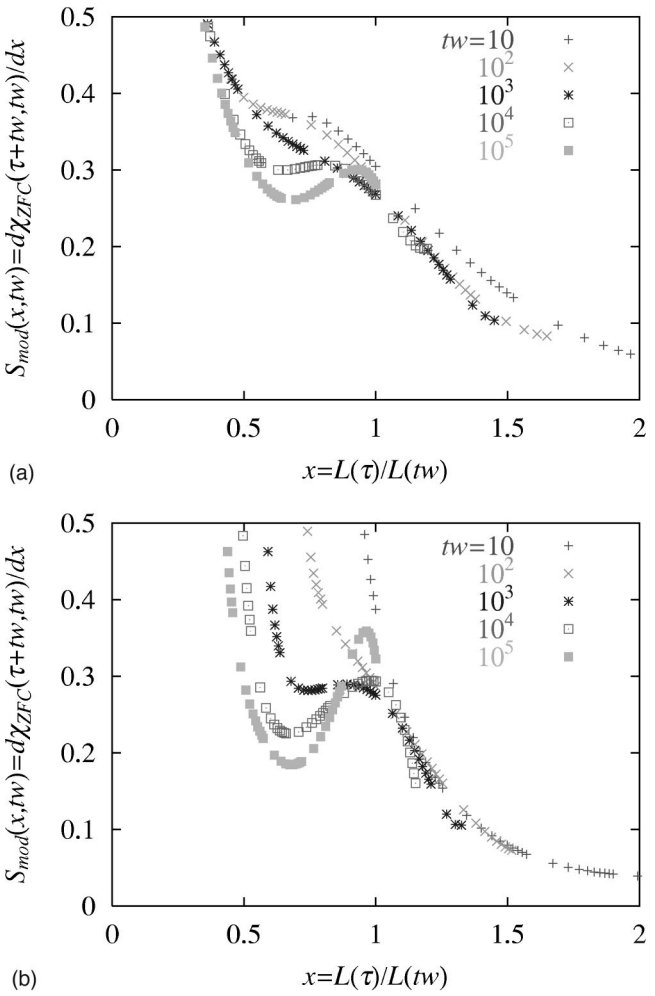

FIG. 20. Scaling plot of the modified relaxation rate function $S_{\mathrm{mod}}(x,t_w)$ at $T/J=1.2$ (upper figure) and 0.8 (lower figure).

with c''' being a numerical constant defined in Eq. (84). In Fig. 21 we show the sum $(T/J)\chi_{\mathrm{ZFC}}(\tau+t_w,t_w)+(T/J)\chi_{\mathrm{TRM}}(\tau+t_w,t_w)$ plotted against $L(t=\tau+t_w)^{-\theta}$ using $\theta=0.82$.[25] We have checked that they satisfy the sum rule (9) and agrees with $(T/J)\chi_{\mathrm{ZFC}}(t,0)$ (see Fig. 12). As can be seen in the figure, the data are indeed consistent with the expected scaling form being linear with $1/L(\tau)^{\theta}$ and pointing toward a constant in the limit $L(\tau)\to\infty$. From the linear fit shown in the figure we find the values of the dynamical susceptibility $(T/J)\chi_D$ as 0.54 at $T/J=1.2$ and 0.33 at $T/J=0.8$. The corresponding dynamical order parameter q_D can be determined via FDT $(T/J)\chi_D=1-q_D$ (60) as 0.46 at $T/J=1.2$ and 0.67 at $T/J=0.8$.

In the analysis of Sec. VII C, we have obtained the value of the equilibrium EA order parameter q_{EA} from which we readily find the equilibrium susceptibility $(T/J)\chi_{\mathrm{EA}}=1-q_{\mathrm{EA}}$. Interestingly enough we find the data of $(T/J)\chi_D(t,0)$ shown in the figure clearly goes over the static susceptibility $(T/J)\chi_{\mathrm{EA}}$ and the anticipated inequality $\chi_{\mathrm{FC}}=\chi_D>\chi_{\mathrm{EA}}$ holds [see Eq. (86)]. This is one of the main results of the present numerical simulation.

The sum rule (9) requires us to examine only either the TRM or ZFC susceptibility plus the growth of the ZFC susceptibility with zero waiting time $\chi_{\mathrm{ZFC}}(t,0)$ which was obtained above. We have already analyzed the ZFC susceptibil-

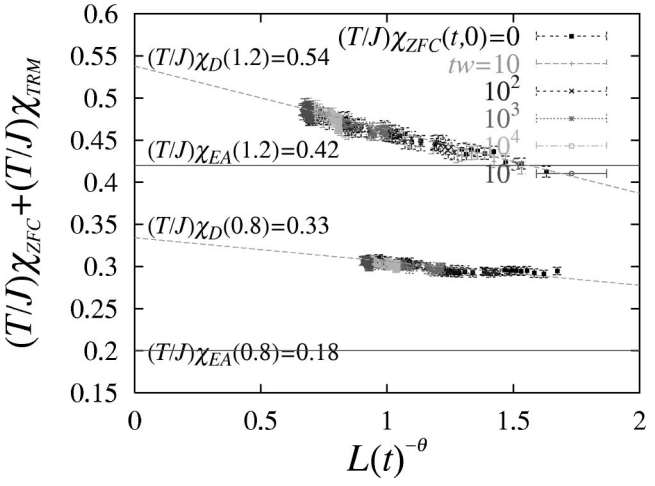

FIG. 21. Growth of the sum $(T/J)\chi_{\mathrm{ZFC}}(\tau+t_w,t_w)+(T/J)\chi_{\mathrm{TRM}}(\tau+t_w,t_w)$ with t. The data is the same as those used in Fig. 12. The fitting lines are due to Eq. (83).

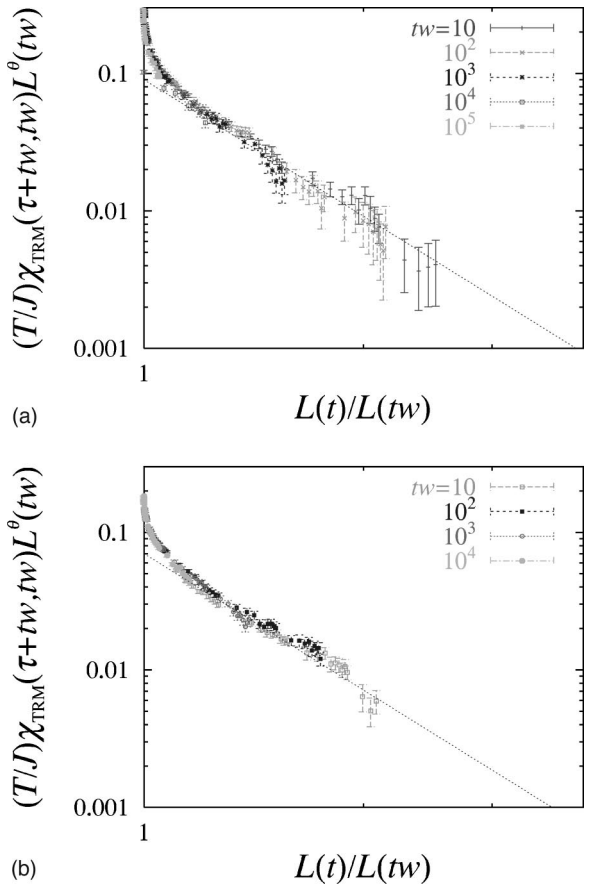

FIG. 22. Scaling plot of $(T/J)\chi_{\rm TRM}(\tau+t_w,t_w)$ at $T=1.2$ (upper figure) and $T=0.8$ (lower figure). The dotted line is a power law fit with exponent $\lambda=3.5$.

ity in the quasiequilibrium regime and crossover regime in the preceding sections. In the following, we examine the TRM susceptibility in the aging regime which will complete our scaling analysis of the linear susceptibilities.

Let us examine the scaling ansatz (87) which reads

$$\chi_{\rm TRM}(\tau+t_w,t_w)\sim c_{\rm nst}\frac{m^2}{\Upsilon[L(t_w)/L_0]^{\theta}}\left(\frac{L(t)}{L(t_w)}\right)^{-\lambda}$$

for the TRM decay in the aging regime $L(\tau)/L(t_w)>1$. In Fig. 22, we show the scaling plot of the the decay of the TRM susceptibility $\chi_{\rm TRM}$ using the stiffness exponent $\theta=0.82$.[25] The results indeed agrees very well with the prediction (87) anticipated by Fisher and Huse[15] and gives the nonequilibrium exponent $\lambda\sim3.5$. The latter satisfies the bound (76) with $d=4$. To our knowledge this is the first time that this fundamental scaling law is confirmed.

F. Separation of the break points of TTI and FDT

The results of the analysis presented so far supports well the existence of the anticipated asymptotic regimes displayed in Figs. 2 and 3 which predicts separation of the breaking of TTI and FDT. In order to look more directly on the separation, we present the ZFC linear susceptibility

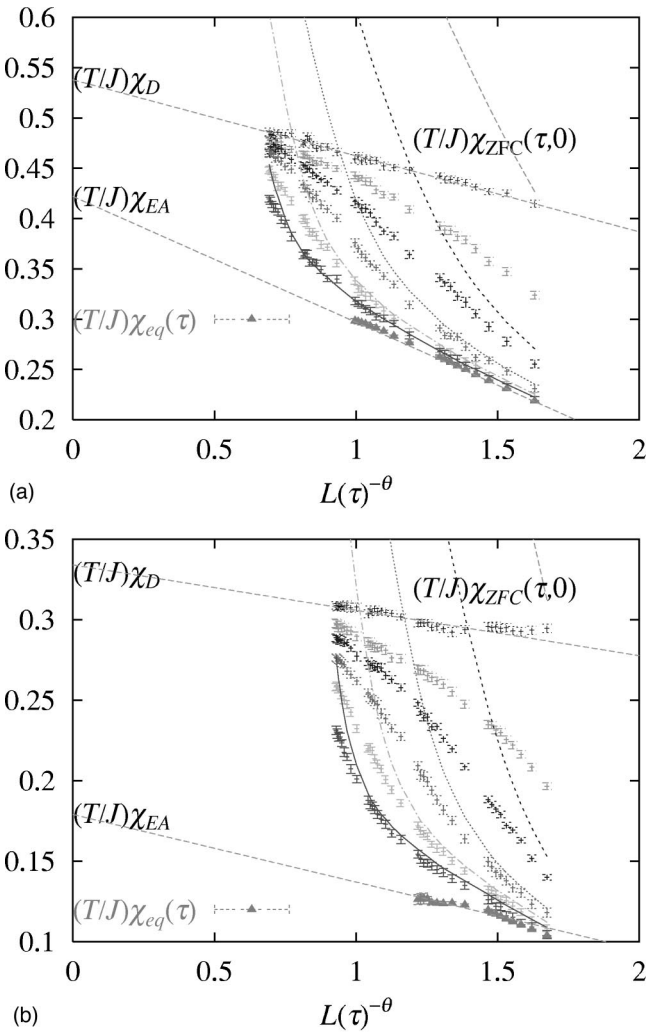

FIG. 23. ZFC linear susceptibilities vs $1/L^{\theta}(\tau)$ at $T/J=1.2$ and $T/J=0.8$. The curves with small symbols are $\chi_{\rm ZFC}(\tau+t_w,t_w)$ with $t_w=0,10,10^2,10^3,10^4,10^5$ from the top to the bottom. The curves with solid lines are $1-C(\tau+t_w,t_w)$ of $t_w=0,10,10^2,10^3,10^4,10^5$ from the top to the bottom. The data of $T\chi_{\rm eq}(\tau)$ (filled triangle) and its linear fit are shown at the bottom. The linear fit to $T\chi_{\rm ZFC}(\tau,0)$ is also shown at the top.

$(T/J)\chi_{\rm ZFC}(t,t_w)$ and spin autocorrelation function $1-C(t,t_w)$ of various waiting times t_w plotted against $1/L(\tau)^{\theta}$ in Fig. 23.

In the figure, we included the equilibrium ZFC linear susceptibility $(T/J)\chi_{\rm eq}(\tau)$ for comparison. The latter was obtained by the FDT $(T/J)\chi_{\rm eq}(\tau)=1-C_{\rm eq}(\tau)$ using the equilibrium spin autocorrelation function $C_{\rm eq}(\tau)$ extracted previously in Sec. VII C. Since $C_{\rm eq}(\tau)$ is a linear function of $1/L(\tau)^{\theta}$ as we confirmed in Sec. VII C (see Fig. 17), $(T/J)\chi_{\rm eq}(\tau)$ becomes a straight line in the plot pointing toward the equilibrium susceptibility $(T/J)\chi_{\rm EA}$. The top curve is $(T/J)\chi_{\rm ZFC}(\tau,0)$ which is at the other extreme: zero waiting time. It becomes also a straight line in the plot as we already saw in Sec. VII E (see Fig. 21) pointing toward the dynamical susceptibility $(T/J)\chi_D$ which is significantly larger than the equilibrium susceptibility $(T/J)\chi_D$.

Note that the slope of the susceptibility in the zero waiting time limit is smaller than that of the equilibrium limit. This can be explained as the following. From Eq. (66), the slope of the equilibrium limit is expected to be proportional to c defined in Eq. (54) while Eq. (83) suggests the slope of the zero waiting time limit is proportional to $c'''=A(1)-c_{\rm nst}$ given in Eq. (84). Here $c_{\rm nst}$ is a positive constant and the value of $A(1)$ can be evaluated by Eq. (57). The latter implies $A(1)<c$ because the first term in Eq. (57) becomes identical to c defined in Eq. (54) while the second term is negative because $\Upsilon/\Upsilon_{\rm eff}[y]\geqslant 1$. Thus we expect $c>c'''$.

Now a surprising observation is that the break points of FDT moves further away from the equilibrium curve by increasing t_w. It appears very unlikely that the break points of the FDT converge to the equilibrium susceptibility $(T/J)\chi_{\rm EA}$. This feature strongly suggests that the violation of TTI and FDT do not take place simultaneously but separates asymptotically. In our scenario presented in Sec. IV E the anomalously extended FDT regime is attributed to the soft droplets. It satisfies FDT but is absent in the ideal equilibrium where there are no frozen-in extended defects: it is a dynamical object.

G. Integral violation of FDT

Let us finally examine the integral violation of the FDT defined in Eq. (23). In Fig. 24, the integral violation $I(\tau+t_w,t_w)$ obtained using our data is plotted against $L(\tau)/L(t_w)$. We see it decreases with increasing waiting time t_w deep in the quasiequilibrium regime $x=L(\tau)/L(t_w)\ll 1$ and increases deep in the aging regime $x=L(\tau)/L(t_w)\gg 1$.

The intriguing problem is the validity of the FDT in the crossover regime $x=L(\tau)/L(t_w)\sim 1$. In Sec. IV E 3 we conjectured that it is satisfied in the crossover regime. In Fig. 24, one can see that the integral violation is indeed decreasing with increasing t_w at $L(\tau)/L(t_w)\sim 1$ which appears compatible with our expectation.

As noted in Sec. IV E 3, a possible scaling variable for the interior of the crossover regime would be $\alpha=\tau/t_w$. In the limit $t_w\to\infty$, possible limits classified by different α are all smashed into the crossover regime $x=L(\tau)/L(t_w)=1$. In Fig. 25, we show the integral violation against $\alpha=\tau/t_w$. Indeed, it is decreasing function for any value of $\alpha=\tau/t_w$ including even the highest α within our data. These observations are compatible with our conjecture that the FDT is asymptotically valid in the crossover regime.

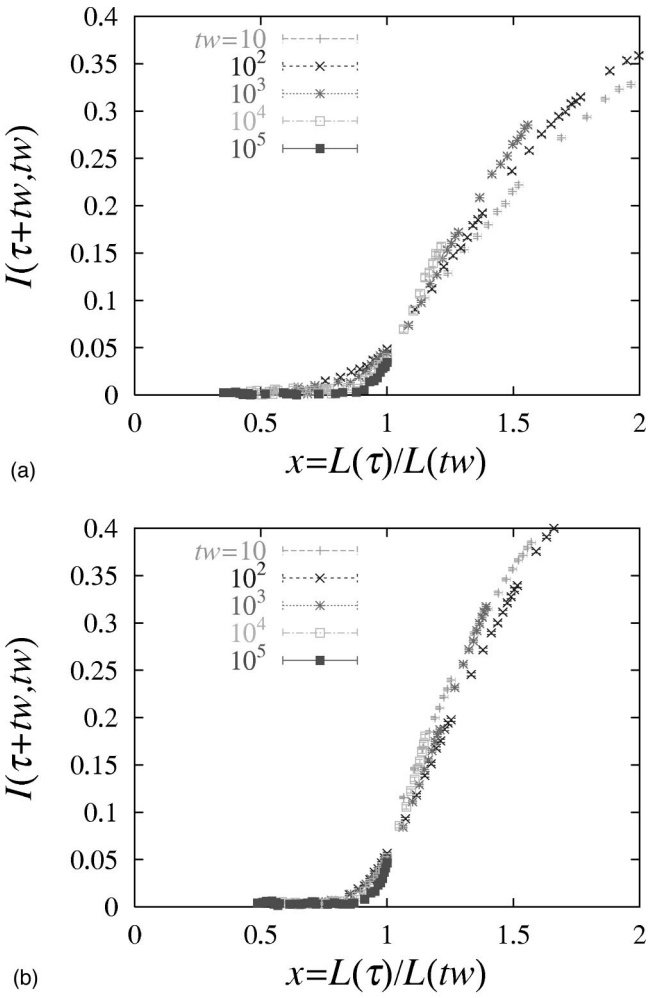

FIG. 24. Integral violation of FDT at $T/J=1.2$ (upper figure) and $T/J=0.8$ (lower figure) plotted against $L(\tau)/L(t_w)$.

VIII. DISCUSSION AND SUMMARY

To summarize, we have presented the results of a detailed MC simulation of a 4D EA Ising spin-glass model in the present paper. We demonstrated that the results can be well understood within the extended droplet theory we proposed recently.[12]

We demonstrated the dynamical susceptibility χ_D larger than the equilibrium susceptibility $\chi_{\rm EA}$ exists in agreement with the extended droplet theory. Within the latter scenario, the two different limits emerge as different large time (size) limits of the two-time (length) quantities. This phenomenon is presumably intimately related with the well known experimental observation $\chi_{\rm FC}>\chi_{\rm EA}$ which has been known for a long time since the very discovery of spin glasses.[9] The question was, if it is a short time transient phenomena or not. The dynamical MFT was the first which clearly appreciated that the difference $\chi_{\rm FC}-\chi_{\rm EA}$ (called ''anomaly''[8]) exists in a well-defined large time limit. Our scaling theory provides systematic extrapolation scheme to obtain the two susceptibilities in a controlled way. It will be certainly interesting to perform such an analysis in experiments and numerical simulations.

We found evidences of the abrupt change of the two-time quantities in the crossover regime $L(\tau)\sim L(t_w)$ which was anticipated in the extended droplet theory. This is directly related to the existence of the two different susceptibilities mentioned above. In previous experimental studies, it was well known that the relaxation rate $S(\tau,t_w)$ has a broad peak as a function of τ at around $\tau\sim t_w$. This phenomenon is expected to be intimately related with the abrupt changes in the crossover regime. We proposed a modified relaxation rate $S_{\rm mod}(x,t_w)$ with $x=L(\tau)/L(t_w)$. As expected, it was found numerically to develop a peak at $x\sim 1$ which sharpens with

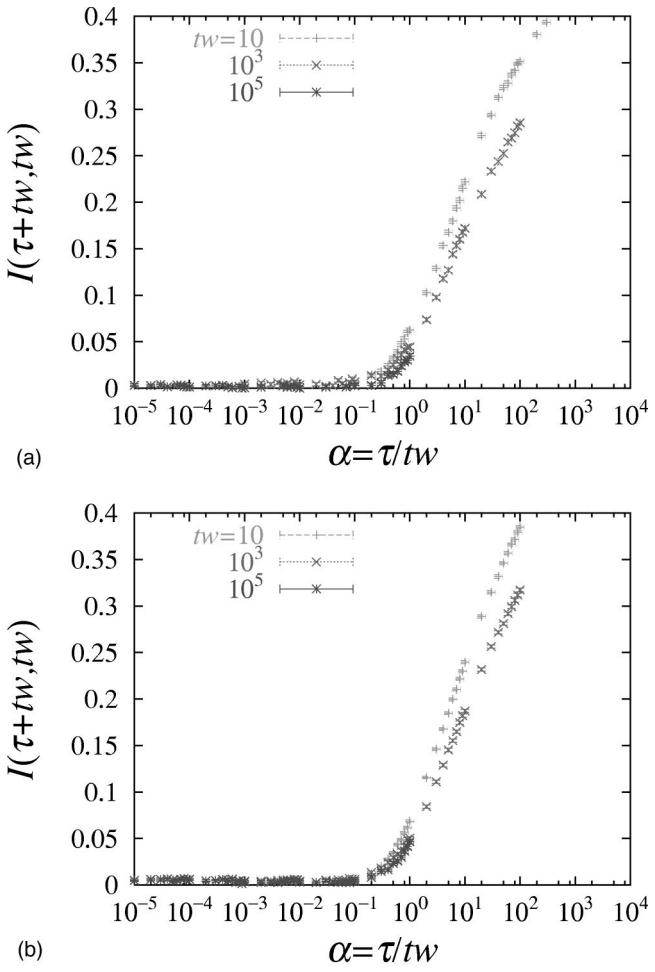

FIG. 25. Integral violation of FDT at $T/J=1.2$ (upper figure) and $T/J=0.8$ (lower figure) plotted against τ/t_w.

increasing t_w when plotted against x. Probably the latter will be more useful in future studies.

A very important feature of our analysis is the two-stroke strategy. In numerical simulations one can obtain directly the data of dynamical length scale $L(t)$ by which time-dependent quantities are immediately translated into length-dependent quantities. In addition, the information of the stiffness exponent θ and fractal dimension d_f of droplets are known from independent studies of equilibrium properties. Thus we had virtually zero fitting parameter left for us in this stage to test various data collapse expected from the scaling ansatz.

The analysis of the growth law itself can be done separately. We found that the growth law $L(t)$ measured at various temperatures below T_c shows the anticipated crossover from short time (length) critical dynamics to asymptotic activated dynamics. In our scaling analysis, we used the critical exponents ν, z and the critical temperature T_c determined in previous studies on equilibrium critical properties so that we have only one free-parameter ψ which was found to be $2.5-3$ in the present model. All the temperature dependences are renormalized into the crossover length $L_0(T)$ and the corresponding crossover time scale $\tau_0(T)\propto L_0(T)^z$ by which all data are collapsed onto a universal growth law function. The latter becomes the expected power law for the critical dynamics at short times (length) and a slower function at large times (length) suggesting activated dynamics.

Similar analysis should be done on experimental studies[52] and numerical simulations of other systems, particularly for 3D models, as well. In experiments, however, this two-stroke strategy is not possible and probably the best way is to start from simplest quantities such as relaxation of the ac susceptibility[19] to work out the parameters of the growth law. The advantage of the experiment, on the other hand, is that one can explore the order of 100 lattice spacings while the present numerical simulations are limited to $1-10$ lattice spacings.

Concerning the effects of critical fluctuation, many recent studies have pointed out the importance to renormalize its effect. In three dimensions, previous results on the growth law by numerical simulations[22,50,53] as well as experiments[54] are well fitted to a power law as $L(t)\sim t^{1/z(T)}$ where the exponent $1/z(T)$ is proportional to T [but this T linearity of $1/z(T)$ starts to break in the temperature range around $T\sim 0.75T_c$ (Ref. 22)]. Probably it is a sort of interpolation formula between T_c, where critical fluctuations are dominant, and $T\to 0$, where all time scales associated with thermally activated processes diverge. Indeed a recent experiment in 3D systems[19] suggests the logarithmic growth law works well if critical fluctuation is properly considered. A recent numerical study of the growth law[20] has also found a signature of the crossover.

It is useful to note that the empirical power law $L(t)\sim t^{1/z(T)}$, combined with the scaling laws in terms of $L(t)$, explains many of the empirical formulas proposed in previous experiments and numerical studies in a unified manner being consistent with our two-stroke approach. For example a fitting formula $C_{\rm eq}(\tau)=q_{\rm EA}+1/\tau^{\alpha}$ used in previous numerical studies (for example, Ref. 60) can be understood as a variant of Eq. (65) with $\alpha=\theta/z(T)$. The well-known ''subaging'' scaling for the TRM susceptibility[5,55] $\chi_{\rm TRM}(\tau+t_w,t_w)\sim F(\tau/t_w^{\mu})$ with $\mu<1$ can be understood as a variant of Eq. (87) with $\mu=1-\theta/\lambda$. The ''ωt scaling'' of the ac susceptibility[5] can also be understood similarly as already noted in a numerical study[23] and an experimental[19] study. In addition, some apparent subaging feature of ac and dc susceptibilities can be removed by considerations of finiteness of cooling rates in real experiments.[19,20,56]

The fundamental assumption of our scenario is that the effective stiffness constant $\Upsilon_{\rm eff}$ of the free-energy gap $F^{\rm typ}_{L,R}$ of droplets is a function of the ratio $x=L/R$ of the two length scales, namely, the length scale of the droplet itself L and of the extended defect R which surrounds the droplet. Most importantly we assumed the vanishing of the effective stiffness constant as $x\to 1$. This allowed the emergence of the two different order parameters $q_{\rm EA}$ and q_D and the associated susceptibilities $\chi_{\rm EA}$ and χ_D. It is desirable to clarify the scaling of the stiffness constant explicitly in the whole range of $0<x<1$.

We expect our conjecture is consistent with the results of recent studies of low-energy excitations in spin-glass

models.[16] In spin glasses of finite sizes R, it is likely that the existence of boundaries will intrinsically induce certain defects as compared with infinite systems.[22,46,47] Then we expect droplet excitations as large as the system size itself $L \sim R$ is anomalously soft. Such an anomaly is indeed found in the series of recent studies.[16] Although there new exponent $\theta'=0$ was conjectured,[16] we consider it is better to attribute this to the zero stiffness constant $\Upsilon_{\rm eff}[1]=0$ as in Eq. (43). The stiffness exponent $\theta>0$, on the other hand, is associated with a defect in Γ as we adopt in Eq. (41). The anomalously low energy and large scale excitations at $L \sim R$ explains the apparently nontrivial overlap distribution function $P(q)$ found in numerous numerical studies of finite size systems[48,49] which appear very similar to the prediction of the equilibrium mean-field theory.[57] Although the meaning of the apparently nontrivial (and probably non-self-averaging) $P(q)$ in equilibrium is not obvious,[58] we consider the contribution of the anomalous excited states to the macroscopic magnetic susceptibility in the present dynamical situation, which is the realistic situation, is very important. As we discussed in Sec. IV E 7, our scenario implies the average overlap $\overline{q}=\int_0^1 dqqP(q)$ measured in equilibrium of finite size systems R (with built-in defects) is equivalent to the dynamical order parameter q_D. We found the latter is related to the field cooled susceptibility $\chi_{\rm FC}$ as $\chi_{\rm FC}=\chi_D=(1-q_D)/k_BT$ [see Eqs. (60) and (86)]. It would remind one of a folklore found in some literature that the difference of $\chi_{\rm FC}$ and $\chi_{\rm ZFC}$ is *somewhat* related to difference of $\overline{q}$ and $q_{\rm EA}$ which is a consequence of the non trivial $P(q)$ found in Parisi's replica symmetry broken solution of the mean-field model.[57] However, we still have to recall the intrinsically dynamical nature of the situation: the domain walls, which allow the anomalous softening of droplets, are dynamical objects and they should be absent in ideal equilibrium where $P(q)$ will have only one delta peak at $q=q_{\rm EA}$ as predicted by the original droplet theory.[14]

Concerning the dynamical MFT, a serious problem in practice is that correction terms to the asymptotic limit is not known. They should obviously exist in the $C-\chi$ relation since the curves in Fig. 14 systematically moves with increasing t_w. Such a feature exists in the data of a recent experiment of simultaneous magnetic noise/response measurement[52] and previous numerical studies.[53,59–61]

Our numerical results indeed suggests the separation of the breaking of TTI and FDT (see Fig. 23). Such a feature has not been realized in previous studies.[52,53,59–61] Within the scaling theory, the correction terms to the expected asymptotic limit (Figs. 2 and 3) themselves are predicted to have salient universal scaling properties which are amenable to be examined in practice. Our numerical results were well explained by the latter scaling ansatz including the decay of the TRM susceptibility (87) which itself was predicted by the original droplet theory more than a decade ago.

ACKNOWLEDGMENTS

This work was supported by a Grant-in-Aid for Scientific Research Program (Grant No. 12640367), and by a Grant-in-Aid for the Encouragement of Young Scientists (Grant No. 13740233) from the Ministry of Education, Culture, Sports, Science and Technology of Japan. The present simulations have been performed on Fujitsu VPP-500/40 at the Supercomputer Center, Institute for Solid State Physics, the University of Tokyo.

*Electronic address: yoshino@ess.sci.osaka-u.ac.jp
†Electronic address: hukusima@issp.u-tokyo.ac.jp
‡Electronic address: takayama@issp.u-tokyo.ac.jp

[1] L.C.E. Struik, *Physical Aging in Amorphous Polymers and Other Materials* (Elsevier, Amsterdam, 1978).
[2] *Spin Glasses and Random Fields*, edited by A.P. Young (World Scientific, Singapore, 1998).
[3] P. Nordblad and P. Svedlindh, in *Spin Glasses and Random Fields* (Ref. 2).
[4] E. Vincent, J. Hammann, and M. Ocio, in *Recent Progress in Random Magnets* (World Scientific, Singapore, 1992).
[5] E. Vincent, J. Hamman, M. Ocio, J.-P. Bouchaud, and L. F. Cuglinadolo, in *Proceeding of the Sitges Conference on Glass Systems*, edited by E. Rubi (Springer, Berlin, 1996).
[6] H. Rieger, in *Annual Review of Computational Physics II*, edited by D. Stauffer (World Scientific, Singapore, 1995).
[7] J.-P. Bouchaud, L. F. Cugliandolo, J. Kurchan, and M. Mézard, in *Spin Glasses and Random Fields* (Ref. 2).
[8] L.F. Cugliandolo and J. Kurchan, Phys. Rev. Lett. **71**, 173 (1993); J. Phys. A **27**, 5749 (1994); Philos. Mag. B **71**, 501 (1995); S. Franz and M. Mézard, Europhys. Lett. **26**, 209 (1994); Physica A **209**, 1 (1994); L.F. Cugliandolo and P. Le Doussal, Phys. Rev. E **53**, 1525 (1996); L.F. Cugliandolo, J. Kurchan, and P. Le Doussal, Phys. Rev. Lett. **76**, 2390 (1996); A. Barrat, R. Burioni, and M. Mézard, J. Phys. A **29**, 1311 (1996).
[9] S. Nagata, P.H. Keeson, and H.R. Harrison, Phys. Rev. B **19**, 1633 (1979).
[10] L.F. Cugliandolo, J. Kurchan, and L. Peliti, Phys. Rev. E **55**, 3898 (1997).
[11] L.F. Cugliandolo and J. Kurchan, J. Phys. Soc. Jpn. **69**, 247 (2000).
[12] H. Yoshino, K. Hukushima, and H. Takayama, cond-mat/0202110 (unpublished).
[13] A.J. Bray and M.A. Moore, Phys. Rev. Lett. **58**, 57 (1987).
[14] D.S. Fisher and D.A. Huse, Phys. Rev. B **38**, 386 (1988).
[15] D.S. Fisher and D.A. Huse, Phys. Rev. B **38**, 373 (1988).
[16] J. Houdayer and O.C. Martin, Europhys. Lett. **49**, 794 (2000); F. Krazakala and O.C. Martin, Phys. Rev. Lett. **85**, 3013 (2000); M. Palassini and A.P. Young, *ibid.* **85**, 3017 (2000).
[17] K. Hukushima, H. Yoshino, and H. Takayama, Prog. Theor. Phys. Suppl. **138**, 568 (2000).
[18] V. Dupis, E. Vincent, J.-P. Bouchaud, J. Hammann, A. Ito, and H.A. Katori, Phys. Rev. B **64**, 174204 (2001).
[19] P.E. Jönsson, H. Yoshino, P. Nordblad, H. Aruga Katori, and A. Ito, Phys. Rev. Lett. **88**, 257204 (2002).
[20] L. Berthier and J.-P. Bouchaud, Phys. Rev. B **66**, 054404 (2002).
[21] D.A. Huse, Phys. Rev. B **43**, 8673 (1990).
[22] T. Komori, H. Yoshino, and H. Takayama, J. Phys. Soc. Jpn. **68**, 3387 (1999).
[23] T. Komori, H. Yoshino, and H. Takayama, J. Phys. Soc. Jpn. **69**, 1192 (2000).

[24] T. Komori, H. Yoshino, and H. Takayama, J. Phys. Soc. Jpn. **69**, 228 (2000).
[25] K. Hukushima, Phys. Rev. E **60**, 3606 (1999).
[26] E. Marinari and F. Zuliani, J. Phys. A **32**, 7447 (1999).
[27] L.W. Bernardi and I. Campbell, Phys. Rev. B **56**, 5271 (1997).
[28] A.K. Hartmann, Phys. Rev. E **60**, 5135 (1999).
[29] A.K. Hartmann, Phys. Rev. E **59**, 84 (1999); A.J. Bray and M.A. Moore, J. Phys. C **17**, L463 (1984); W.L. McMillan, Phys. Rev. B **30**, 476 (1984).
[30] L. Lundgren, P. Nordblad, and L. Sandlund, Europhys. Lett. **1**, 529 (1986); P. Nordblad, L. Lundgren, and L. Sandlund, *ibid.* **3**, 235 (1987); R. Mathieu, P.E. Jönsson, D.N.H. Nam, and P. Nordblad, Phys. Rev. B **63**, 092401 (2001).
[31] L.F. Cugliandolo, J. Kurchan, and F. Ritort, Phys. Rev. B **49**, 6331 (1994).
[32] L.F. Cugliandolo, D.S. Dean, and J. Kurchan, Phys. Rev. Lett. **79**, 2168 (1997).
[33] S. Franz, M. Mézard, Giorgio Parisi, and Luca Peliti, Phys. Rev. Lett. **81**, 1758 (1998).
[34] D.A. Huse and D.S. Fisher, Phys. Rev. B **35**, 6841 (1987).
[35] A.J. Bray, Adv. Phys. **43**, 357 (1994).
[36] L.F. Cugliandolo and D.S. Dean, J. Phys. A **28**, 4213 (1995).
[37] H. Bokil, B. Drossel, and M.A. Moore, Phys. Rev. B **62**, 946 (2000); Phys. Rev. Lett. **81**, 4252 (1998).
[38] Unfortunately the ambiguity of the width $\ln a$ is unavoidable within the independent droplet model.
[39] M. Ocio, H. Bouchiat, and P. Monod, J. Phys. (France) Lett. **46**, L647 (1985); J. Magn. Magn. Mater. **54-57**, 11 (1986).
[40] Ph. Refregier, M. Ocio, J. Hammann, and E. Vincent, J. Appl. Phys. **63**, 4343 (1988).
[41] L. Berthier, J.-L. Barrat, and J. Kurchan, Eur. Phys. J. B **11**, 635 (1999).
[42] We thank Ludovic Berthier for pointing out this excessive response due to thermalized domain walls in usual coarsening systems. See Ref. 41.
[43] L. Lundgren, P. Svendlindh, P. Nordblad, and O. Beckman, Phys. Rev. Lett. **51**, 911 (1983).
[44] J.-O. Anderson, J. Mattson, and P. Svendlindh, Phys. Rev. B **46**, 8297 (1992).
[45] A. Barrat and L. Bertheir, Phys. Rev. Lett. **87**, 087204 (2001).
[46] C.M. Newman and D.L. Stein, Phys. Rev. E **57**, 1356 (1998).
[47] A. Middleton, Phys. Rev. Lett. **83**, 1672 (1999).
[48] H.G. Katzgraber, M. Palassini, and A.P. Young, Phys. Rev. B **63**, 184422 (2001), and references therein.
[49] E. Marinari, G. Parisi, F. Ricci-Tersenghi, J.J. Ruiz-Lorenzo, and F. Zuliani, J. Stat. Phys. **98**, 973 (2000), and references therein.
[50] J. Kisker, L. Santen, M. Schrenckenberg, and H. Rieger, Phys. Rev. B **53**, 6418 (1996).
[51] M. Palassini and A.P. Young, Phys. Rev. Lett. **85**, 3017 (2000).
[52] D. Hérisson and M. Ocio, Phys. Rev. Lett. **88**, 257202 (2002).
[53] E. Marinari, G. Parisi, F. Ricci-Tersenghi, and J.J. Ruiz-Lorenzo, J. Phys. A **31**, 2611 (1998).
[54] Y.G. Joh, R. Orbach, G.G. Wood, J. Hammann, and E. Vincent, Phys. Rev. Lett. **82**, 438 (1999).
[55] M. Ocio, M. Alba, and J. Hammann, J. Phys. (Paris) **41**, 1335 (1980); M. Alba, M. Ocio, and J. Hammann, Europhys. Lett. **2**, 45 (1986).
[56] V.S. Zotev, G.F. Rodriguez, R. Orbach, E. Vincent, and J. Hammann, cond-mat/0202269 (unpublished).
[57] For the review see *Spin Glass Theory and Beyond*, edited by M. Mézard, G. Parisi, and M. Virasoro (World Scientific, Singapore, 1987).
[58] C.M. Newman and D.L. Stein, Phys. Rev. Lett. **87**, 077201 (2001).
[59] S. Franz and H. Rieger, J. Stat. Phys. **79**, 749 (1995).
[60] G. Parisi, F. Ricci-Tersenghi, and J.J. Ruiz-Lorenzo, J. Phys. A **29**, 7943 (1996).
[61] F. Ricci-Tersenghi, F. Ritort, and M. Picco, Eur. Phys. J. B **21**, 211 (2001).